JOURNAL OF GEOPHYSICAL RESEARCH, VOL. 102, NO. D14, PAGES 16,697–16,713, JULY 27, 1997

A split-window algorithm for land surface temperature from advanced very high resolution radiometer data: Validation and algorithm comparison

César Coll and Vicente Caselles

Department of Thermodynamics, Faculty of Physics, University of Valencia, Valencia, Spain

Abstract. A split-window algorithm for deriving land surface temperatures (LSTs) from advanced very high resolution radiometer (AVHRR) channels 4 and 5 is proposed and validated with in situ measured temperatures. On the basis of the radiative transfer theory the algorithm defines a set of surface-independent coefficients which are equivalent to the classical split-window coefficients for sea surface temperature (SST). These coefficients are calculated using SST matchups (coincident AVHRR and buoy measurements) provided by the National Oceanic and Atmospheric Administration (NOAA)-NASA Pathfinder Database of worldwide measurements. Thus calibration of the split-window coefficients is done using real data. The variability of atmospheric attenuation is represented in the proposed algorithm by a quadratic dependence on the brightness temperature difference. For LST determination the emissivity effect is modeled through an additive coefficient which depends on surface emissivity in the AVHRR channels 4 and 5. The algorithm is validated for both SST and LST by using independent ground-based and AVHRR data. The database used in the validation of LST was obtained for a wide range of surface types in a semiarid environment. The same databases are used to compare the accuracies of other published split-window algorithms. The proposed algorithm yields standard errors of temperature estimate between ±1.0 and ±1.5 K, and no significant biases are observed. Although results are encouraging, more validation is required principally for moist atmospheric conditions.

1. Introduction

Land surface temperatures (LSTs) derived from the advanced very high resolution radiometer (AVHRR) instrument onboard the National Oceanic and Atmospheric Administration (NOAA) satellites provide a unique tool for deriving regional fluxes of latent and sensible heat over land surfaces [*Norman et al.*, 1995]. For this purpose, LST needs to be corrected for the absorption and emission of the Earth's atmosphere and the nonblackness of natural emitting surfaces. Split-window methods for atmospheric correction, which use channels 4 (10.3–11.3 μm) and 5 (11.5–12.5 μm) of the AVHRR 2, perform well when applied to the recovery of sea surface temperature (SST) [*McClain et al.*, 1985], giving accuracies of ±0.5 K for most atmospheric conditions [*May*, 1993]. The split-window technique takes advantage of the differential absorption between AVHRR channels 4 and 5, which is closely correlated with atmospheric conditions, mainly given by the water vapor and air temperature profiles [*McMillin*, 1975].

The effect of surface emissivity is superimposed onto the atmospheric attenuation in the case of land. Unlike sea surface, land surface thermal emission is highly variable because it depends on a large number of factors: pixel composition, vegetation cover, soil background, and surface geometry, among others. Moreover, there is evidence of a spectral variation of surface emissivity for different land surface materials [*Salisbury and D'Aria*, 1992]. This spectral and spatial dependence means that the correlation between the radiances measured in different channels is modified in such a manner that is not correlated to the atmospheric properties, the modification being highly dependent on the nature of the surface. In the last years a number of papers have addressed the extension of the split-window technique to the recovery of LST, resulting in a considerable variety of approaches and theoretical algorithms [e.g., *Price*, 1984; *Becker and Li*, 1990; *Sobrino et al.*, 1991; *Ottlé and Vidal-Madjar*, 1992; *Prata*, 1993; *Coll et al.*, 1994]. In general, LST split-window algorithms take the form of linear combinations of the satellite brightness temperatures; however, different expressions and values have been proposed for the algorithm coefficients.

Both sea and land surface algorithms have been derived from the radiative transfer theory assuming certain approximations. The theoretical development determines the functional form of the split-window algorithms. However, there is an important difference between SST and LST algorithms with regard to the methodology in which the coefficients are derived. For sea surface these coefficients are obtained empirically using extensive data sets of in situ measured SSTs and cotemporal, collocated AVHRR measurements (the so-called matchups). The coefficients are then obtained by statistical regression [*Strong and McClain*, 1984]. The matchup database consists of high-quality, cloud-free measurements distributed over worldwide oceans. This methodology ensures that the algorithms are calibrated with real data and over a high variety of atmospheric conditions. Each time new matchup data are available, algorithms can be further validated and regularly updated.

For land surface an empirical methodology cannot be ap-

Paper number 97JD00929.
0148-0227/97/97JD-00929$09.00

plied easily due to the lack of an appropriate database. This database should include quality in situ measurements of surface temperature and concurrent satellite data for a wide range of surface types (soils, crops, forests, grasslands, semiarid surfaces with sparse vegetation, etc.) and atmospheric situations of different water vapor content. Empirical algorithms have been attempted using a very limited amount of data [*Vidal*, 1991; *Kerr et al.*, 1992]. Their applicability to different atmospheric and surface conditions still needs to be tested. An alternative methodology consists in obtaining the split-window coefficients from synthetically calculated databases [*Becker and Li*, 1990; *Ottlé and Vidal-Madjar*, 1992; *Sobrino et al.*, 1994]. In that case a radiative transfer model must be used with varied atmospheric profiles and surface conditions (temperatures and emissivities). However, it is a difficult task to reproduce the worldwide variability. Besides, the results depend on the radiative transfer model employed, which is subject to errors in the parameterization of atmospheric absorption processes, especially that of the water vapor in the 10–13 μm window (continuum absorption). Moreover, split-window coefficients can be very sensitive to the physical conditions simulated. Results may change significantly when cases are added or removed from the data set [*Wan and Dozier*, 1989]. It is also possible to include unrealistic cases which may bias the regression analysis.

In any case, the various LST algorithms proposed have not been sufficiently validated with ground-truth data; neither have the absolute attainable accuracies in LST been estimated. The reason is mainly the inherent difficulty of obtaining in situ temperature measurements comparable to satellite measurements. *Prata* [1994a] has identified such difficulties and devised and carried out a field experiment with the purpose of providing data sets suitable for LST algorithm testing. Full tabulation of the data has been published by *Prata* [1994b], which constitutes the most extensive LST data set available at present (more than 350 matchups). Measurements include different types of surface: bare and fallow agricultural soils, wheat crops, and pasture lands in a semiarid region of southeast Australia characterized by dry atmospheric conditions. We have used this data set to validate the split-window algorithm proposed in this paper and to compare the results of the most significant published algorithms.

2. Objectives

The objectives of this paper can be summarized as follows: (1) to derive a split-window algorithm for LST determination using AVHRR data, (2) to validate the derived algorithm using in situ temperature measurements, and (3) to compare the performance of various published split-window algorithms. Section 3 gives a brief description of the theoretical split-window model used, which was derived by *Coll et al.* [1994]. In addition, a new parameterization of the emissivity effect in terms of surface temperature and atmospheric humidity has been included. The algorithm defines a set of surface-independent coefficients which are equivalent to the classical split-window coefficients for the blackbody surface; therefore they can be calculated from regression analysis over actual sea surface data. To this end, we have used the extensive, worldwide SST data set compiled by the NOAA-NASA Pathfinder Matchup Database [*Podestá et al.*, 1995] in section 4. Therefore the calculated atmospheric coefficients are calibrated with actual data covering worldwide atmospheric situations. In section 5 the proposed algorithm has been validated using in situ and AVHRR matchups from two sources: (1) an independent SST database from the Centre de Météorologie Spatiale, Lannion, France and (2) the aforementioned LST database of *Prata* [1994b], which is useful for validating both the atmospheric and emissivity effects on the temperature retrieval. These two databases are then used in section 6 for a comparison between split-window algorithms. Finally, the discussion and the conclusion of the work are given.

3. Split-Window Algorithm for Land Surface Temperature

In this section we briefly describe a theoretical split-window model for LST retrieval from AVHRR data. Later, a methodology is proposed and justified for deriving the split-window coefficients of the model by using SST matchups.

3.1. Theoretical Model

The split-window model used in this paper has been given already by *Coll et al.* [1994]. The inputs it requires are the mean surface emissivity in AVHRR channels 4 and 5, $\varepsilon = (\varepsilon_4 + \varepsilon_5)/2$, and the spectral emissivity difference in these channels, $\Delta\varepsilon = \varepsilon_4 - \varepsilon_5$. It can be written as

$$T = T_4 + A(T_4 - T_5) + \Delta + B(\varepsilon) \tag{1}$$

where T is the actual LST, T_4 and T_5 are the brightness temperatures in channels 4 and 5, and

$$A = \frac{1 - \tau_4(\theta)}{\tau_4(\theta) - \tau_5(\theta)} \tag{2}$$

$$\Delta = -[1 - \tau_5(\theta)]A(T_{a4}^{\uparrow} - T_{a5}^{\uparrow}) \tag{3}$$

$$B(\varepsilon) = \alpha(1 - \varepsilon) - \beta\Delta\varepsilon \tag{4}$$

$$\alpha = (b_4 - b_5)A\tau_5(\theta) + b_4 \tag{5}$$

$$\beta = A\tau_5(\theta)b_5 + \alpha/2 \tag{6}$$

$$b_i = \frac{T_i}{n_i} + \gamma_i\left(\frac{n_i - 1}{n_i}T_i - T_{ai}^{\downarrow}\right)[1 - \tau_i(0°)] \qquad i = 4, 5 \tag{7}$$

with $\tau_i(\theta)$ being the atmospheric transmittance for channel i ($i = 4, 5$) and zenith observation angle θ; $T_{ai}^{\uparrow}(T_{ai}^{\downarrow})$ being the effective atmospheric temperatures for channel i in the upward (downward) direction [see *McMillin*, 1975]; $n_4 = 4.667$, $n_5 = 4.260$ for NOAA 11 AVHRR [*Sobrino et al.*, 1991]; and $\gamma_i \approx 1.6$ is the ratio of the hemispheric downwelling sky radiance to π times the directional radiance at nadir [*Schmugge et al.*, 1991].

Equations (2) and (3) are the classical coefficients derived for a blackbody surface [*McMillin*, 1975; *Maul*, 1983]. If emissivity is high, as it is for most natural surfaces in the 10–12.5 μm window, coefficients A and Δ only depend on the atmospheric properties and not on the surface emissivity. They will be called hereafter atmospheric split-window coefficients. As a consequence, A and Δ can be applied to any type of surface, provided that the emissivity effects are compensated by the term $B(\varepsilon)$ (equation (4)). This term is a linear function of the mean emissivity ε and the spectral difference $\Delta\varepsilon$. However, the corresponding coefficients α and β (equations (5) and (6)) depend on the atmospheric properties through $T_{ai}^{\downarrow}$, τ_i (due to the reflection of the downwelling sky radiance), coefficient A, and surface temperature through T_i. As shown in section 3.3,

these dependencies can be easily parametrized through coefficients b_i (equation (7)), for which linear expressions on the atmospheric water vapor content (or precipitable water W) and the satellite brightness temperatures T_i have been derived.

3.2. Applicability of SST Data to LST Determination

The main advantage of the above formulation is that the atmospheric coefficients A and Δ do not depend on the surface type, so they can be calculated empirically using the extensive worldwide matchup database available for the sea surface. To this end, the NOAA/NASA Matchup Database [*Podestá et al.*, 1995] is used in section 4. However, some issues must be previously examined before the atmospheric coefficients associated with sea surface can be extrapolated to land surfaces: first, the effect of emissivity of the sea surface (nearly but not exactly a blackbody); second, the differences existing between typical sea and land atmospheres; and third, the bulk-skin temperature difference in SST measurements.

3.2.1. Sea surface emissivity. The sea surface is essentially homogeneous in space, with a emissivity very close to unity and certain spectral variation (it is slightly larger around 11 μm than around 12 μm [*Salisbury and D'Aria*, 1992]). There is also evidence of an angular dependence of the emissivity, especially for zenith angles larger than 30°, as shown in the theoretical calculations of *Masuda et al.* [1988]. According to these calculations we can take $\varepsilon_4 = 0.992$ and $\varepsilon_5 = 0.988$ for NOAA 11 AVHRR and nadir observation. The contribution in the split-window formulation of the $B(\varepsilon)$ term (equation (4)) can be now evaluated. Since the value of $\Delta\varepsilon$ is positive, it can be anticipated that terms in (4) cancel each other out; consequently, coefficient $B(\varepsilon)$ is small. Using the angular values of *Masuda et al.* [1988] and a varied set of atmospheric profiles, *Coll and Caselles* [1994] calculated $B(\varepsilon)$ for the sea surface as a function of the observation angle and the atmospheric humidity. Although large values were obtained for large observation angles, the emissivity effect was found to be negligible for $\theta < 40°$ and to have an average value $B(\varepsilon) = 0.04 \pm 0.15$ K. As a result, the sea surface can be considered as a blackbody in the split-window formulation. Therefore we can assume $B(\varepsilon) \approx 0$ for $\theta < 40°$, and a regression analysis of $T - T_4$ against $T_4 - T_5$ will yield coefficients A and Δ according to (1).

3.2.2. Marine and land atmospheres. The atmospheric boundary layer is usually coupled to sea surfaces. For land surfaces, however, the surface-atmosphere system is more varied. Particularly, temperature profile inversions are frequent over continental surfaces during clear nights. *Platt and Prata* [1993] have shown that there is a marked effect on $T_4 - T_5$ (negative values of $T_4 - T_5$) when strong inversion exists. Since this situation is not presumably present in SST matchup data, the database is biased in this regard. Additionally, large air-surface temperature differences may be found for the land case, depending on the evaporation rate [*Price*, 1984]. *May and Holyer* [1993] have addressed the impact of air-surface temperature differences on the split-window algorithms. They have shown that the effect is relatively small: typically a variation of 0.15–0.4 K in surface temperature error for each 10 K variation in the air-surface temperature difference. The reason is that the brightness temperature difference $T_4 - T_5$ is itself sensitive to these temperature variations; therefore the correction is implicitly included.

3.2.3. Bulk-skin temperature difference. For heterogeneous, rough land surfaces it is possible to define a radiometric LST which can be measured by satellite radiometers. The LST is a composite temperature obtained from the weighted contributions of the different homogeneous surfaces within the pixel [*Caselles et al.*, 1992; *Becker and Li*, 1995]. In this regard, the composite surface emissivity must be defined consistently in such a way that the laws of radiometry are accomplished. Thus, when studying land surfaces, we will assume that temperature and emissivity are "effective" parameters which allow us to consider the land surface as homogeneous and flat [*Caselles et al.*, 1992].

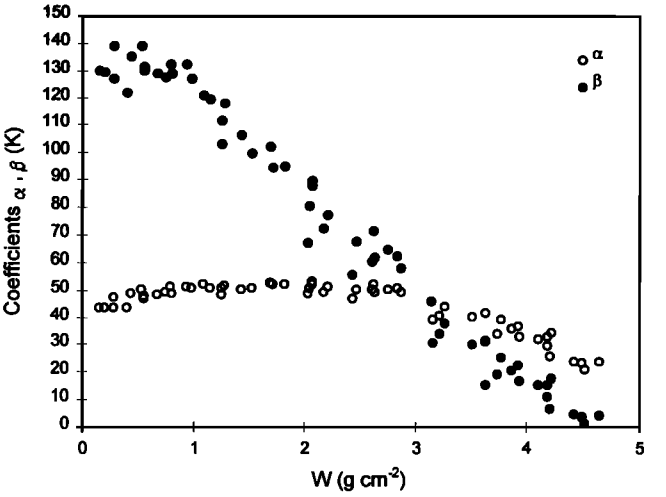

Figure 1. Coefficients α and β as a function of the atmospheric water vapor content W.

In order to extrapolate the SST data to LST retrieval we must ensure that radiometric sea temperatures are used. In situ measurements of sea temperatures are usually performed at depths of typically 1 m (bulk temperature), whereas thermal infrared measurements refer to a thin layer of 10 μm (skin temperature). In the absence of turbulent mixing there can be significant differences between these two temperatures due to two opposite processes: the cooling of the sea skin caused by evaporation and the heating of the surface in high insolation and low wind conditions. As a consequence, the bulk-skin temperature difference may range between +1.0 and −1.0 K, depending on which effect prevails [*Schluessel et al.*, 1990]. In such conditions there is a lack of correlation between the satellite and in situ temperatures, which may have an important effect on the regression analysis. Since we are interested in skin, radiometric temperatures, data with larger bulk-skin effect must be eliminated from the database. A procedure is discussed in section 4 which will be followed to minimize this effect.

3.3. Emissivity Effect on LST

In the application of the split-window equation for LST retrievals the emissivity correction term $B(\varepsilon)$ must be calculated. To do that, the coefficients α and β can be optimized according to the atmospheric properties and the surface temperature. Figure 1 plots values of such coefficients versus atmospheric water vapor content W for different atmospheric profiles and surface temperatures. It is shown that α is roughly constant with values around 50 K for most cases, whereas β decreases linearly with atmospheric moisture. A new parameterization is suggested in terms of W and T_i to provide a more accurate determination of the emissivity coefficients. To do

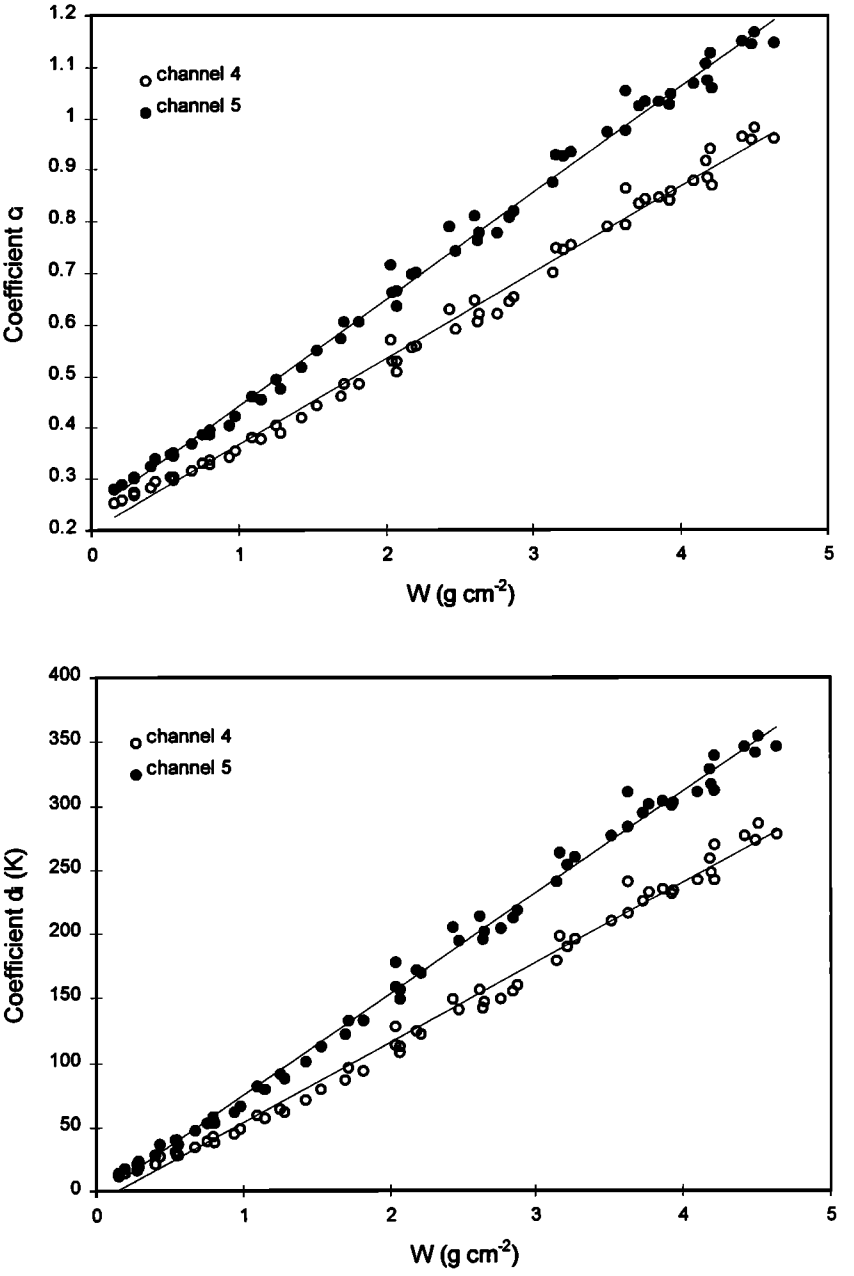

Figure 2. Coefficients c_i and d_i (equation (8)) as a function of the atmospheric water vapor content W. The solid lines are the linear regression fits.

that, it should be noted that the coefficients b_i (equation (7)) can be expressed as a linear function of T_i:

$$b_i = c_i(W)T_i - d_i(W) \tag{8}$$

with c_i and d_i being linear functions of W as shown in Figure 2 using the same data as in Figure 1. From these results we have

$$b_4 = (0.198 + 0.167W)T_4 - (62.3W - 10) \tag{9}$$

$$b_5 = (0.234 + 0.206W)T_5 - (78.9W - 5) \tag{10}$$

with W given in grams per square centimeter and an error of estimate of 3 K for b_i.

As shown in (5) and (6), the atmospheric transmittance in channel 5, τ_5, and the atmospheric coefficient A are also required in the formulation. Atmospheric transmittances decrease with atmospheric moisture, and an approximate linear relationship could be used for τ_5. The next section will address what value must be given to the coefficient A. Therefore α and β can be estimated for a particular area as functions of the brightness temperatures if a measure of the water vapor content or climatological data are available. If such data are not available, mean climatological values can be used for α and β according to Figure 1.

4. Analysis of Sea Surface Temperature Data

In this section we use the NOAA 11 AVHRR matchup database compiled within the NASA-NOAA Pathfinder project to calculate the atmospheric coefficients A and Δ. The

Pathfinder Matchup Database (PFMDB) is available through the Physical Oceanography Distributed Active Archive Center (PODAAC) at NASA's Jet Propulsion Laboratory. The database consists of separated files containing information of the satellite and in situ measurements, which is organized by satellite and year. For the present work, we use the NOAA 11 database of years 1988–1993 in its currently available version (version 18). The steps involved in the PFMDB compilation, the summary of its composition, and the magnitudes included are fully described by *Podestá et al.* [1995]. The geographic and temporal distribution of the data includes a wide range of atmospheric and oceanic conditions. In situ measurements are obtained from different networks of moored and drifting buoys distributed over the worldwide oceans within latitudes 60°N and 60°S. The satellite data are extracted in 5 × 5 pixel boxes centered at each in situ location, and the matchup is only completed if the in situ measurement and satellite overpass times are within a ±30-min window and within a distance of 10 km. A very important step in the data processing is the elimination of cloud-contaminated data. For this purpose, two successive filtering schemes involving several threshold and spatial uniformity tests are applied to the matchup data. In the present analysis, we have only used the data that passed both filters to ensure high quality of the matchups (typically 30% of the data).

In addition to the filtering procedures applied in the database compilation, we have only selected the data which fit our purposes. For this reason, we have rejected all the matchups with a zenith observation angle $\theta > 40°$. This filtering is done to minimize the emissivity effect in the split-window algorithm since $B(\varepsilon) \approx 0$ for angles $\theta < 40°$ as discussed in the previous section. A further threshold is applied which intends to eliminate bulk-skin temperature differences which may affect the matchups. In the processing of the database a first-guess SST is calculated using a version of the NOAA/NESDIS operational Nonlinear SST (NLSST) algorithm [*Walton et al.*, 1990]. The difference between the first-guess and the in situ temperature measurement is also used in the database as a filtering test. Only if this difference is less than ±2 K, the test is passed. However, this difference can be due to the bulk-skin effect since it typically produces a lack of correlation between the satellite and the buoy temperatures. To minimize this effect, we have applied a much more restrictive difference threshold of ±0.5 K.

The above criteria are then used to extract the matchup data from the original database. Descriptive statistics of the selected database are given in Table 1, which show the average, the standard deviation, and the range of variation of the in situ measured temperatures T, the difference $T - T_4$, and the satellite brightness temperature difference $T_4 - T_5$. In general, similar values have been found for all selected years. The surface temperatures range from 0° to 30°C approximately, whereas $T - T_4$ (which basically represents the atmospheric attenuation) takes values between 0° and 8°C. The difference $T_4 - T_5$ shows much less variability, ranging roughly from 0° to 3°C.

A regression analysis of $T - T_4$ against $T_4 - T_5$ has been performed according to (1). If a linear regression is used, the slope of the regression yields the split-window coefficient A of (1), whereas coefficient Δ is given by the offset term. However, these coefficients are dependent on the atmospheric conditions [see *Coll et al.*, 1994]; therefore the split-window equation will be no longer lineal for global scale algorithms. To account for this nonlinearity, several approaches can be adopted. *Walton* [1988] proposed the Cross Product SST algorithm (CPSST), which is a modification of the differential absorption principle. *Walton et al.* [1990] derived the Nonlinear SST (NLSST) algorithm using a different approach. Both nonlinear algorithms are being presently applied as NOAA operational algorithms. However, they are specifically derived for SST and cannot be extended to LST retrievals. Another possibility consists in separating the database according to several smaller ranges of the brightness temperature difference $T_4 - T_5$ and then deriving optimized linear algorithms for such interval. As a disadvantage, this procedure can introduce discontinuities in the boundaries of the $T_4 - T_5$ intervals.

Table 1. Descriptive Statistics for the Selected NOAA 11 Matchup Data

Year	Number of Data	T, °C	$T - T_4$, °C	$T_4 - T_5$, °C	δT, °C
1988	367	18.4 (6.7)	2.6 (1.4)	1.1 (0.6)	−0.1 ± 0.3
		[5.2, 30.0]	[0.2, 7.3]	[0.1, 2.8]	[−0.98, 0.88]
1989	2156	19.0 (7.1)	2.6 (1.5)	1.1 (0.6)	−0.1 ± 0.3
		[0.4, 30.8]	[0.1, 7.8]	[0.0, 2.9]	[−1.17, 1.13]
1990	2408	19.8 (7.0)	2.8 (1.6)	1.2 (0.6)	−0.1 ± 0.3
		[0.4, 31.8]	[0.2, 7.8]	[0.0, 2.9]	[−1.35, 1.16]
1991	2268	18.5 (7.2)	2.6 (1.5)	1.1 (0.6)	0.0 ± 0.3
		[−0.3, 31.0]	[0.2, 8.0]	[0.0, 2.8]	[−1.38, 1.16]
1992	2507	21.9 (6.0)	3.4 (1.6)	1.3 (0.6)	0.1 ± 0.3
		[0.6, 31.7]	[0.1, 7.9]	[0.0, 3.0]	[−0.99, 1.24]
1993	4602	22.1 (5.6)	3.3 (1.5)	1.4 (0.6)	0.0 ± 0.3
		[1.4, 31.8]	[0.2, 8.3]	[0.0, 3.1]	[−1.28, 1.11]

The average, the standard deviation (in parens), and the range of variation (in brackets) are given. T is the in situ SST measurement, T_4 and T_5 are the AVHRR channels 4 and 5 data, and δT is the temperature error when the split-window equation for year 1993 is applied.

An alternative approach consists in maintaining the structure of (1) to introduce the atmospheric dependence of the split-window coefficients by simply assuming a quadratic split-window algorithm in $T_4 - T_5$ as proposed by *Coll et al.* [1994]. Figure 3 shows a plot of $T - T_4$ versus $T_4 - T_5$ for data of the year 1991, which reveals the quadratic dependence of the data distribution. Then, a parabolic regression analysis will yield the coefficient A as a linear function of $T_4 - T_5$ and the coefficient Δ as the constant offset. For all the years studied the results of the statistical regression are very similar. We have chosen the largest data set (year 1993) to derive the split-window coefficients. The rest of the data sets have been used to check the consistency of these derived coefficients. For year 1993 we have obtained

$$A = 1.34 + 0.39(T_4 - T_5)$$

$$\Delta = 0.56 \text{ K}$$

with an estimate error (root-mean-square deviation (rmsd)) $\sigma = 0.3$ K and a coefficient of determination $r^2 = 0.948$. Then, the SST split-window equation takes the form $T = T_4 + [1.34 + 0.39(T_4 - T_5)](T_4 - T_5) + 0.56$. This equation was also applied to the data sets corresponding to the years 1988–1992, and the statistics of the differences between the in situ measurements and the algorithm-derived SSTs were calculated and shown in the last column of Table 1. We can see that the algorithm has an optimum performance, with standard deviations of 0.3 K for all the years and biases between −0.1 and 0.1 K. The mean differences and standard errors are small

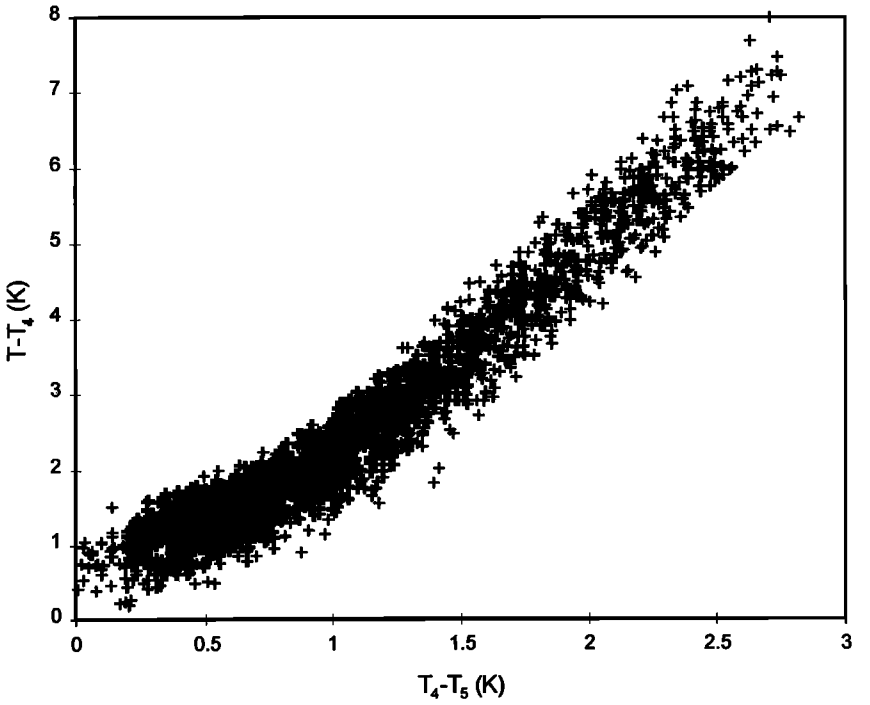

Figure 3. Plot of $T - T_4$ against $T_4 - T_5$ for the 1991 matchup database. T is the in situ SST measurement; T_4 and T_5 are the AVHRR temperatures in channels 4 and 5.

enough to give a good confidence margin to the coefficients obtained; nevertheless, a more complete validation is carried out in the next section which includes LST data sets.

As a comparison, a linear regression for the 1993 data set yields $A = 2.46$, $\Delta = -0.11$ K, $\sigma = 0.4$ K, and $r^2 = 0.935$. The results are worse than those of the quadratic equation, although it may be argued that the improvement introduced by that approach is not very important. In Figure 4 the differences between the actual and the predicted SST, δT, as obtained from the quadratic (Figure 4a) and linear fits (Figure 4b) are plotted against $T_4 - T_5$. The data in the figure correspond to the year 1991. We can see that δT depends on $T_4 - T_5$ in the linear approach, whereas it is nearly independent in the quadratic case. For instance, if we select data with $T_4 - T_5 < 0.5$ K (dry atmospheric conditions), we obtain $\delta T = 0.4 \pm 0.3$ K in the linear case, but $\delta T = 0.0 \pm 0.3$ K for the quadratic case. Additionally, for $T_4 - T_5 > 2.5$ (humid atmospheres), the results are $\delta T = 0.4 \pm 0.5$ K and $\delta T = 0.0 \pm 0.5$ K, respectively. This example shows that the linear approach may underestimate the surface temperatures by about 0.4 K in certain conditions. Since LST split-window algorithms are usually applied for regional studies with restricted atmospheric situatio ıs, we propose the quadratic approach in order to avoid systematic errors or biases in the retrieved temperatures.

To end this section, we must stress that the quadratic approach is not the most accurate algorithm for SST recovery. In fact, the NLSST algorithm (which is included in the PFMDB files) yields $\sigma = 0.2$ K and errors ranging from -0.5 to $+0.5$ K (by definition of our database selection). However, our interest is not SST retrieval, and the NLSST algorithm cannot be extrapolated to land surfaces. For land surfaces, emissivity errors are the most important source of error in split-window algorithms [*Caselles et al.*, 1997a]. Since the total error in split-window derived LSTs is dominated by the emissivity uncertainty, the accuracy of the quadratic algorithm is sufficient.

5. Validation

The algorithm proposed for LST determination is

$$T = T_4 + [1.34 + 0.39(T_4 - T_5)](T_4 - T_5) + 0.56 + \alpha(1 - \varepsilon) - \beta\Delta\varepsilon \quad (11)$$

where the coefficients α and β can be optimized in terms of the atmospheric water vapor content and the surface brightness temperatures (equations (5), (6), (9), and (10)) or taken as climatological mean values. In this section we have used different data sets of in situ measured temperatures and coincident AVHRR data in order to validate the proposed algorithm. Two different data sets have been used: (1) the SST matchup database from the Centre de Météorologie Spatiale (CMS), Lannion, France, comprising 347 situations collected over European seas, which has been used as an independent source for testing the atmospheric correction part of the algorithm and (2) the LST database collected by *Prata* [1994a, b] over different land surface types, with a total of 358 coincident in situ and AVHRR measurements, which allows the validation of both atmospheric and emissivity effects together.

5.1. Data Set Description

For all the validation data sets used in this study, basic statistics including mean value, standard deviation, and range of variation are given in Table 2. The quantities shown are the in situ measured temperatures T, the difference $T - T_4$ (which gives the atmospheric and emissivity correction), and the satellite brightness temperature difference $T_4 - T_5$. In

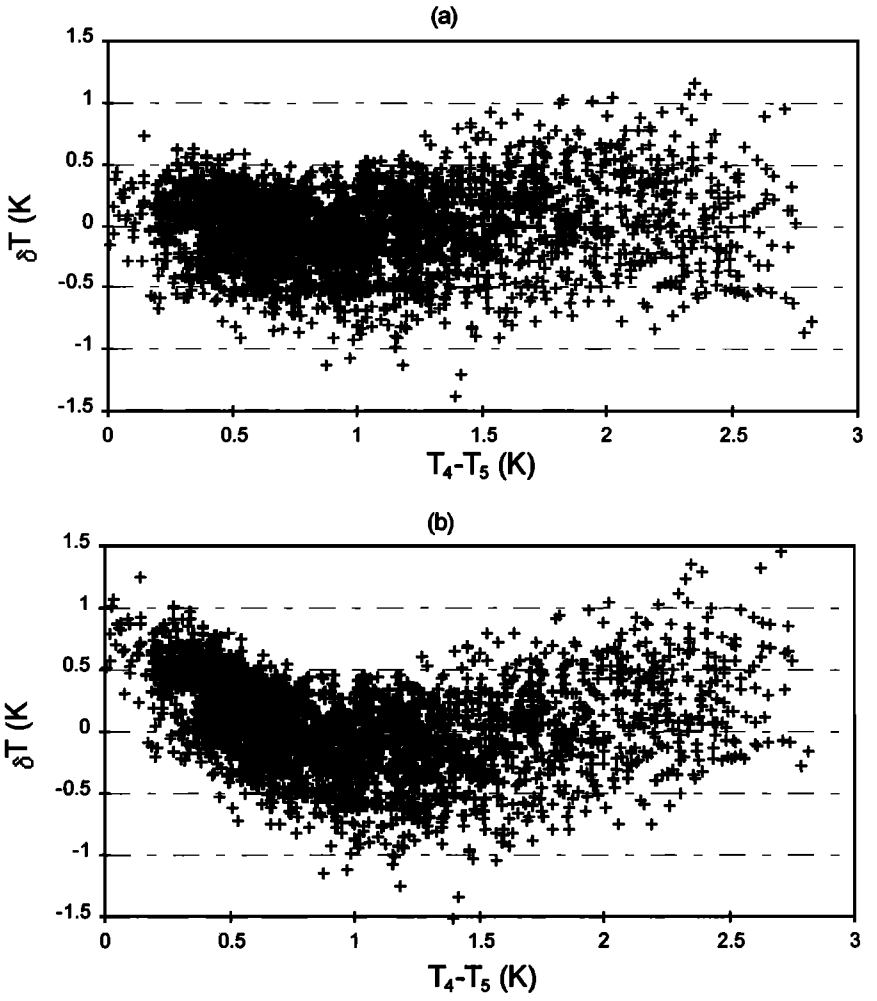

Figure 4. Error in temperature δT (in situ SST minus algorithm-derived temperature) for the 1991 data as a function of the brightness temperature difference $T_4 - T_5$. (a) Quadratic split-window equation. (b) Linear split-window equation.

addition, the last columns show the results from two different linear regression analysis performed over the data sets, including the rmsd error (σ), the range of the error, and the coefficient of determination r^2. The LR column is a linear regression of $T - T_4$ against $T_4 - T_5$, according to the equation $T = T_4 + A(T_4 - T_5) + B$. The MR column is a linear multiple regression of $T - T_4$ against T_4 and T_5 separately, resulting in the equation $T = aT_4 + bT_5 + c$. It is aimed to study the correlation between the correction and the satellite temperatures independently, rather than the brightness temperature differences. The results of Table 2 indicate that the coefficient of determination is always greater for the MR than for the LR analysis (due to the one more degree of freedom), although the resulting temperature errors are quite similar. This shows that the temperature difference $T_4 - T_5$ is the main correcting factor for the split-window technique. The errors of estimate for the regression analysis (σ) shown in Table 2 can be regarded as the maximum accuracies that can be obtained with simple split-window algorithms, as they have been optimized by minimization for the corresponding data sets. These values are useful as reference for evaluating the performance of the theoretical split-window equations.

The CMS SST database is composed of NOAA 11 AVHRR and in situ data collected over the Mediterranean Sea and the North Atlantic Ocean during years 1989–1990 [see *Antoine et al.*, 1992]. Table 2 shows temperate features and lower variability if compared with those of the PFMDB (Table 1). It is interesting to check the ability of the global algorithm of (11) to adapt itself to the more restricted midlatitude conditions of the CMS SST database.

Prata [1994a] has described in detail the experimental approach devised to collect the LST database. Full tabulation of the data has been published by *Prata* [1994b]. Two field sites of about 1 km^2 (comparable to the AVHRR pixel size at nadir) were selected in southeast Australia. Both sites were flat, with uniform terrain and low atmospheric water vapor content (about 1 g/cm^2). With the LST database the suitability of the split-window coefficients derived from SST matchups will be checked. On the other hand, the parameterization of the emissivity correction proposed in section 3 will be validated for several surface covers. Low humidity implies large values for coefficient β (see Figure 1), which makes the emissivity effect larger, particularly that of the emissivity difference $\Delta\varepsilon$. The Walpeup site is a large wheat field, and data were collected for three different successive states of the surface: bare soil, wheat crop, and fallow. The Hay site is a semiarid pasture land, the type of surface being unchanged during the experiment. For the Walpeup-fallow and Hay-pasture land sites, both NOAA

Table 2. Descriptive Statistics for the Validation Data Sets

Data Set	Number of Data	T, °C	$T - T_4$, °C	$T_4 - T_5$, °C	LR	MR
Lannion SST	347	15.3 (4.5) [4.4, 27.4]	2.3 (0.9) [−0.5, 5.4]	1.0 (0.3) [−0.2, 2.0]	σ = 0.6°C [−1.4, 1.8] r^2 = 0.632	σ = 0.5°C [−1.6, 1.5] r^2 = 0.709
Walpeup-fallow	118					
NOAA 11/day	26	26.0 (8.0) [14.5, 42.1]	5.0 (2.6) [1.6, 12.1]	1.5 (1.0) [0.0, 4.3]	σ = 0.9°C [−2.0, 1.8] r^2 = 0.881	σ = 0.9°C [−1.7, 1.8] r^2 = 0.883
NOAA 11/night	32	6.9 (3.9) [1.2, 16.6]	1.9 (1.3) [−1.4, 4.0]	−0.2 (0.5) [−0.9, 0.8]	σ = 1.0°C [−2.5, 1.9] r^2 = 0.378	σ = 1.0°C [−2.5, 1.9] r^2 = 0.392
NOAA 12/morning	35	11.2 (5.7) [1.7, 22.9]	2.2 (1.1) [0.2, 4.8]	0.6 (0.5) [−0.5, 1.5]	σ = 0.8°C [−1.4, 1.8] r^2 = 0.452	σ = 0.8°C [−1.5, 1.8] r^2 = 0.470
NOAA 12/evening	25	11.1 (3.9) [4.7, 18.8]	3.2 (1.3) [0.7, 5.7]	0.4 (0.5) [−0.6, 1.3]	σ = 0.7°C [−1.7, 1.2] r^2 = 0.718	σ = 0.7°C [−2.0, 0.9] r^2 = 0.776
Hay-pasture land	113					
NOAA 11/day	22	23.6 (8.5) [13.4, 45.7]	5.1 (1.6) [3.2, 8.0]	1.0 (0.9) [−0.1, 3.0]	σ = 0.9°C [−1.2, 1.9] r^2 = 0.715	σ = 0.8°C [−1.2, 2.0] r^2 = 0.761
NOAA 11/night	34	5.8 (5.8) [−0.8, 22.1]	2.5 (0.8) [1.0, 4.0]	−0.4 (0.3) [−1.1, 0.4]	σ = 0.8°C [−1.4, 1.5] r^2 = 0.020	σ = 0.8°C [−1.5, 1.4] r^2 = 0.070
NOAA 12/morning	33	7.3 (6.8) [−1.2, 23.6]	2.1 (0.8) [0.5, 3.6]	0.1 (0.5) [−0.7, 1.5]	σ = 0.7°C [−1.3, 1.5] r^2 = 0.160	σ = 0.7°C [−1.3, 1.5] r^2 = 0.167
NOAA 12/evening	24	9.6 (6.3) [1.3, 24.4]	3.9 (1.1) [1.6, 6.3]	0.1 (0.4) [−0.6, 1.1]	σ = 0.9°C [−2.0, 1.5] r^2 = 0.257	σ = 0.9°C [−2.2, 1.2] r^2 = 0.307
Walpeup-bare soil	30					
NOAA 11/day	13	29.9 (8.2) [18.4, 43.0]	5.2 (2.2) [2.4, 10.6]	1.8 (1.0) [0.5, 4.1]	σ = 1.0°C [−1.5, 1.1] r^2 = 0.800	σ = 0.7°C [−1.4, 0.8] r^2 = 0.911
NOAA 11/night	17	9.3 (4.2) [4.0, 17.3]	3.2 (1.1) [1.7, 5.6]	−0.1 (0.4) [−0.6, 0.7]	σ = 0.7°C [−1.6, 1.4] r^2 = 0.627	σ = 0.7°C [−1.6, 1.3] r^2 = 0.639
Walpeup-wheat crop	97					
NOAA 11/day	42	34.5 (10.7) [12.6, 52.9]	6.0 (3.3) [1.1, 13.9]	1.9 (1.0) [0.4, 4.6]	σ = 2.0°C [−3.7, 3.8] r^2 = 0.625	σ = 2.0°C [−3.4, 4.0] r^2 = 0.630
NOAA 11/night	55	7.4 (3.4) [1.5, 18.3]	1.9 (1.5) [−1.7, 7.1]	0.1 (0.4) [−0.6, 1.2]	σ = 1.4°C [−3.3, 3.8] r^2 = 0.100	σ = 1.2°C [−2.9, 2.9] r^2 = 0.417

T is the in situ temperature measurement, and T_4 and T_5 are AVHRR channels 4 and 5 data. The average, the standard deviation (in parens), and the range of variation (in brackets) are given. The LR and MR columns show the results of two regression analysis (see text), showing the standard error of estimate of T (σ), the range of the error, and the coefficient of determination (r^2). LR, linear regression; MR, multiple regression.

11 and 12 data were collected, including the daytime (1500–1700 local solar time (LST)) and nighttime passes (0200–0400 LST) for NOAA 11, and the morning (0600–0800 LST) and evening (1900–2100 LST) passes for NOAA 12. For the Walpeup-bare soil and wheat crop surfaces, only NOAA 11 at daytime and nighttime were obtained.

The in situ temperatures were measured by a number of contact thermometers regularly distributed along the test sites in order to capture the temperature variability. Some were placed over the ground surface to measure the ground temperature T_g, whereas others measured the vegetation temperature T_v attached to the natural vegetation for the Walpeup-fallow and Hay-pasture land sites or placed in the air close to the plant leaves for the wheat crop surface. The data given by *Prata* [1994b] are the average values for T_g and T_v. The composite surface temperature comparable to the satellite measurements is defined as $T = P_v T_v + (1 - P_v)T_g$, with P_v being the proportion of vegetation. For the Walpeup-fallow and Hay-pasture land sites we have taken $P_v = 0.5$, whereas for the Walpeup-bare soil it is $P_v = 0$ [*Prata*, 1994a].

The wheat crop data set was divided into two categories by *Prata* [1994a]: the growing crop and the mature crop. Both the growing (green) and the mature (senescent) wheat plants present high emissivities, and the cavity effect increases further these values and reduces the spectral differences [*Salisbury and D'Aria*, 1992]. *Prata* [1994a] reports field measurements for both wheat crop types showing differences not distinguishable from the experimental errors. According to this it is reasonable to assign a value $\varepsilon = 0.98$ and $\Delta\varepsilon = 0$ for both categories. As for the split-window algorithm validation and comparison, the only parameter which defines the surface is its emissivity; we have considered together the wheat crop data for the present analysis.

The vegetation temperatures T_v were measured with thermometers in contact with the air rather than the plant leaves. Consequently, large differences are found between T_g and T_v

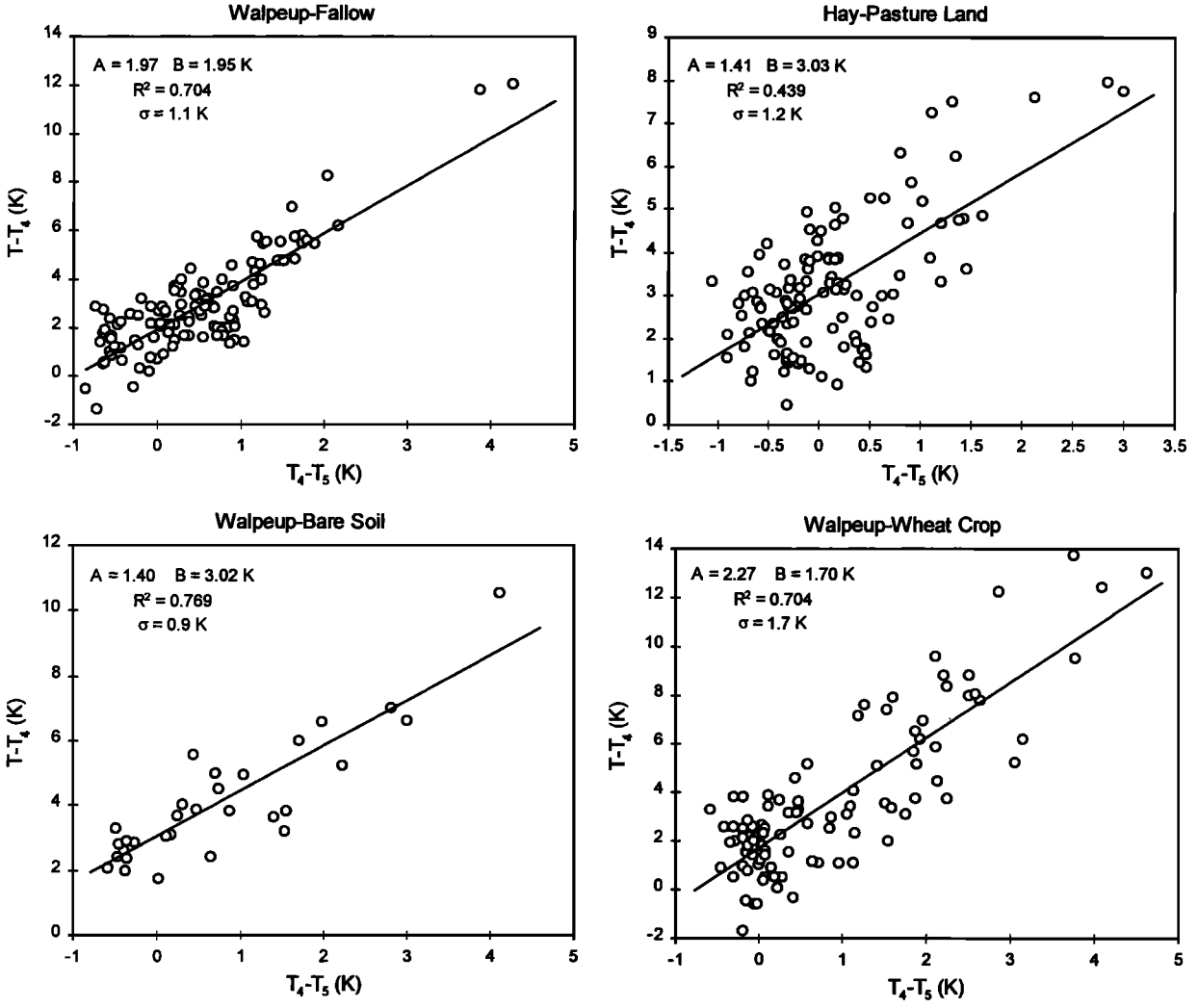

Figure 5. Plot of $T - T_4$ against $T_4 - T_5$ for the four surfaces studied in the LST validation data sets. The solid line is the linear regression according to $T = T_4 + A(T_4 - T_5) + B$. The values of the regression coefficients A and B, the coefficient of determination (R^2), and the standard error of estimate (σ) are shown.

for the daytime data. *Prata* [1994a] proposed to calculate the composite in situ temperature with $P_v = 0.25$ for the growing crop and $P_v = 0.7$ for the mature crop. In the study carried out here, such an assumption yielded misleading results. For the daytime data, $T - T_4$ resulted in a mean value of 2.4°C with a range from −4.6° to 7.2°C. These figures are very low compared with the values for the previous data sets (see Table 2). Besides, the comparison of most split-window algorithms with these data yielded large overestimation up to some 10°C in several cases. For these reasons, we have defined the in situ temperatures as $T = T_g$ for the daytime wheat crop data set. For the nighttime data, T_g and T_v are quite similar, and therefore the composite temperature can be defined as by *Prata* [1994a] with reasonable results. However, the standard errors for both the LR and MR analysis are larger (2°C for the daytime data). It may be a consequence of the inherent difficulty of measuring in situ temperatures for complex surfaces such as a wheat crop.

Figure 5 depicts the correlation between $T - T_4$ and $T_4 - T_5$ for the four surfaces. In Table 2, relevant statistics for the LST data sets have been presented, with the data being grouped by surface type, satellite, and passing time. In the error analysis given by *Prata* [1994a] a maximum error of ±3°C is estimated for the comparison between the in situ and satellite-derived temperatures. The ranges of errors for the LR and MR analysis shown in Table 2 are well within these limits for most of the data sets.

For the Walpeup-fallow data set the highest values in $T - T_4$ and $T_4 - T_5$ (about 12° and 4°C, respectively; see Figure 5) correspond to the highest values in T (up to 40°C (table 2)). Negative values for $T_4 - T_5$ indicate nocturnal inversions in the temperature and humidity profiles [*Platt and Prata*, 1993]. These are found mostly for all nighttime data sets but also for the evening and morning cases. Moreover, negative $T_4 - T_5$ values could also indicate that the surface emissivity is larger in channel 5; that is, $\Delta\varepsilon < 0$.

5.2. Validation Results

In order to apply the proposed split-window algorithm (equation (11)) it is necessary to estimate the coefficients α and β appropriate for each data set and to specify the emissivity values ε and $\Delta\varepsilon$ according to the nature of the different surfaces. For the sea surface we have taken two cases: (1) the blackbody ($\varepsilon = 1$ and $\Delta\varepsilon = 0$) and (2) the theoretical values of

Table 3. Validation Results for the CMS SST Data Set

CMS SST/NOAA 11	$\varepsilon = 1$, $\Delta\varepsilon = 0$	$\varepsilon = 0.99$, $\Delta\varepsilon = 0.004$
This work	0.0 ± 0.6 [−1.5, 1.8]	−0.1 ± 0.6 [−1.6, 1.7]
Price [1984]	−1.0 ± 0.7 [−2.8, 1.0]	−0.6 ± 0.7 [−2.5, 1.4]
Becker and Li [1990]	−1.6 ± 0.6 [−3.1, 0.2]	−1.6 ± 0.6 [−3.1, 0.2]
Vidal [1991]	−0.4 ± 0.6 [−2.0, 1.3]	0.3 ± 0.6 [−1.3, 2.0]
Kerr et al. [1992]	...	...
Ottlé and Vidal-Madjar [1992]	−0.8 ± 0.6 [−2.2, 1.0]	...
Ulivieri et al. [1992]	0.5 ± 0.6 [−1.0, 2.3]	0.3 ± 0.6 [−1.2, 2.1]
Prata [1993]	−0.1 ± 0.6 [−1.6, 1.7]	−0.1 ± 0.6 [−1.6, 1.7]
Sobrino et al. [1994]	...	...
François and Ottlé [1996]/*Q*	0.1 ± 0.7 [−2.7, 2.1]	−0.4 ± 0.7 [−2.8, 1.6]
François and Ottlé [1996]/*W*	...	...

The mean error, the standard deviation, and the range of error are given in degrees Celsius. *Q*, quadratic algorithm in $T_4 - T_5$; *W*, algorithm including water vapor dependent coefficients.

Masuda et al. [1988] ($\varepsilon = 0.99$ and $\Delta\varepsilon = 0.004$). The CMS SST database does not include water vapor measurements, thus constant climatological values have been used for α and β. For midlatitude conditions we have assumed $\alpha = 40$ K and $\beta = 75$ K. The first row of Table 3 displays the results of the comparison, giving the mean value, the standard deviation of the differences (measured minus algorithm temperatures), and the range of variation. For the two surface emissivity cases considered, the results are very similar, showing the small impact expected for the sea surface emissivity.

For the LST data sets the correct specification of the surface emissivity is more important and should be based on actual measurements of emissivity. *Prata* [1994b] includes a few field measurements of emissivity for some surface covers in the Walpeup and Hay test sites. The extrapolation of spot field measurements to the coarse spatial resolution of the AVHRR is still a problem, although several approaches have been proposed [e.g., *Valor and Caselles*, 1996]. However, broad conclusions can be outlined from published laboratory spectra [e.g., *Salisbury and D'Aria*, 1992] and field measurements [*Rubio et al.*, 1997]. For most agricultural soils and vegetated surfaces, $\varepsilon > 0.95$ and $-0.018 < \Delta\varepsilon < 0$ [*Caselles et al.*, 1997b]. The presence of vegetation and cavity effects tend to increase ε and decrease the absolute value of $\Delta\varepsilon$, so that $\varepsilon \approx 0.98$ and $\Delta\varepsilon \approx 0$ can be assumed for vegetation. The values reported by *Prata* [1994b] fall well within these ranges. We have considered the emissivity as independent of the satellite (NOAA 11 or 12) and the overpass time (day, night, morning, or evening), allowing only variations among surface types.

The coefficients α and β have been calculated as a function of the atmospheric humidity and surface temperatures. We have used the mean monthly climatological atmospheric parameters for both test sites given by *Prata* [1994b]. These include the water vapor content W and the atmospheric transmittance τ_5. Since only rough estimates of the atmospheric parameters are necessary, we have taken constant values for all the data sets. We have used $W \approx 1$ g cm^{-2} in (9) and (10) allowing dependence on the brightness temperatures, and $\tau_5 \approx 0.8$ in (5) and (6). The coefficient A required by these last two equations is $A = 1.34 + 0.39(T_4 - T_5)$.

The results of the algorithm validation for the Walpeup-fallow surface are shown in the first row of Table 4, where statistics are given for the four subsets considered. In Table 5 the results are grouped by satellite and finally considered together in the last column. For the Walpeup-Fallow data set we have selected $\varepsilon = 0.98$ and $\Delta\varepsilon = -0.005$ according to *Prata* [1994a]. For the NOAA 11 data the worst result is obtained for the data point with $T_4 - T_5 \approx 4$°C, for which the algorithm

Table 4. Validation Results for the Walpeup-Fallow Data Set

Walpeup-Fallow/ NOAA 11 and 12	$\varepsilon = 0.98$, $\Delta\varepsilon = -0.005$			
	11/Daytime	11/Nighttime	12/Morning	12/Evening
This work	−0.3 ± 1.1 [−3.4, 1.7]	0.2 ± 1.0 [−2.5, 1.9]	−0.8 ± 0.8 [−2.5, 1.0]	0.6 ± 0.7 [−1.2, 1.9]
Price [1984]	−2.4 ± 1.2 [−4.9, 0.1]	0.3 ± 1.2 [−2.1, 3.0]	−2.3 ± 1.2 [−4.6, 1.0]	−0.5 ± 0.9 [−2.0, 1.1]
Vidal [1991]	−1.6 ± 0.9 [−3.5, 0.1]	0.0 ± 1.1 [−2.2, 2.4]	−2.0 ± 1.0 [−4.0, 0.5]	−0.4 ± 0.8 [−1.9, 0.8]
Kerr et al. [1992]	1.3 ± 0.9 [−0.8, 3.1]	2.1 ± 1.1 [−0.1, 4.3]	0.5 ± 0.9 [−1.4, 2.5]	2.0 ± 0.7 [0.4, 3.2]
Ottlé and Vidal-Madjar [1992]	−0.3 ± 1.0 [−2.5, 1.7]	0.1 ± 1.0 [−2.2, 2.1]	−1.3 ± 0.9 [−3.1, 0.5]	0.1 ± 0.7 [−1.6, 1.4]
Ulivieri et al. [1992]	1.1 ± 1.1 [−1.0, 3.5]	1.0 ± 1.0 [−1.4, 2.9]	−0.2 ± 0.8 [−1.8, 1.6]	1.2 ± 0.7 [−0.6, 2.4]
Prata [1993]	−0.6 ± 0.9 [−2.7, 1.2]	0.7 ± 1.1 [−1.5, 2.9]	−1.2 ± 1.0 [−3.1, 1.1]	0.4 ± 0.7 [−1.1, 1.7]
Sobrino et al. [1994]	0.2 ± 1.0 [−2.2, 2.2]	0.8 ± 1.0 [−1.5, 2.9]	−0.7 ± 0.9 [−2.5, 1.2]	0.8 ± 0.8 [−0.9, 2.1]
Becker and Li [1995]	0.0 ± 1.0 [−2.4, 2.1]	0.6 ± 1.0 [−1.8, 2.5]	−0.8 ± 0.9 [−2.7, 1.0]	0.7 ± 0.8 [−1.0, 2.0]
François and Ottlé [1996]/*Q*	−0.3 ± 2.5 [−9.6, 1.9]	1.3 ± 1.1 [−1.5, 2.8]	0.1 ± 0.9 [−1.7, 2.0]	1.6 ± 0.7 [−0.1, 3.0]
François and Ottlé [1996]/*W*	2.5 ± 1.7 [0.0, 6.9]	1.2 ± 1.1 [−1.7, 2.6]	0.6 ± 0.9 [−0.7, 2.4]	1.8 ± 1.0 [−0.3, 3.6]

The mean error, the standard deviation, and the range of error are given in degrees Celsius.

Table 5. Summary of the Validation Results for the Walpeup-Fallow Data Set

Walpeup-Fallow/NOAA 11 and 12 (Summary)	$\varepsilon = 0.98$, $\Delta\varepsilon = -0.005$		
	NOAA 11	NOAA 12	All Data
This work	0.0 ± 1.1	−0.2 ± 1.0	−0.1 ± 1.1
	[−3.4, 1.9]	[−2.5, 1.9]	[−3.4, 1.9]
Price [1984]	−0.9 ± 1.8	−1.5 ± 1.4	−1.2 ± 1.6
	[−4.9, 3.0]	[−4.6, 1.1]	[−4.9, 3.0]
Vidal [1991]	−0.7 ± 1.3	−1.3 ± 1.2	−1.0 ± 1.3
	[−3.5, 2.4]	[−4.0, 0.8]	[−4.0, 2.4]
Kerr et al. [1992]	1.7 ± 1.1	1.1 ± 1.1	1.4 ± 1.1
	[−0.8, 4.3]	[−1.4, 3.2]	[−1.4, 4.3]
Ottlé and Vidal-Madjar [1992]	−0.1 ± 1.0	−0.7 ± 1.1	−0.4 ± 1.4
	[−2.5, 2.1]	[−3.1, 1.4]	[−3.1, 2.1]
Ulivieri et al. [1992]	1.0 ± 1.1	0.4 ± 1.0	0.7 ± 1.1
	[−1.4, 3.5]	[−1.8, 2.4]	[−1.8, 3.5]
Prata [1993]	0.1 ± 1.2	−0.5 ± 1.2	−0.2 ± 1.2
	[−2.7, 2.9]	[−3.1, 1.7]	[−3.1, 2.9]
Sobrino et al. [1994]	0.5 ± 1.1	−0.1 ± 1.1	0.2 ± 1.1
	[−2.2, 2.9]	[−2.5, 2.1]	[−2.5, 2.9]
Becker and Li [1995]	0.3 ± 1.1	−0.2 ± 1.1	0.1 ± 1.1
	[−2.4, 2.5]	[−2.7, 2.0]	[−2.7, 2.5]
François and Ottlé [1996]/*Q*	0.6 ± 2.0	0.7 ± 1.1	0.6 ± 1.6
	[−9.6, 2.8]	[−1.7, 3.0]	[−9.6, 3.0]
François and Ottlé [1996]/*W*	1.8 ± 1.6	1.1 ± 1.1	1.4 ± 1.4
	[−1.7, 6.9]	[−0.7, 3.6]	[−1.7, 6.9]

The mean error, the standard deviation, and the range of error are given in degrees Celsius.

overestimates the measured LST by 3.4°C. For the NOAA 12 data, some inconsistency is found: an overestimation of 0.8°C is obtained for the morning data, whereas for the evening data the algorithm underestimates the in situ temperatures by 0.6°C. As shown in section 6, the large differences between the bias for the two overpass times of NOAA 12 are a common feature of all the split-window algorithms studied.

As an indication of the emissivity effect, we show here the mean values and standard deviations for the coefficients. For the whole data set we have obtained $\alpha = 51 \pm 3$ K and $\beta = 86 \pm 18$ K. From these values, $B(\varepsilon) = 1.5 \pm 0.2$ K. The small standard deviation obtained for $B(\varepsilon)$ indicates that constant mean values can be used for α and β.

In order to specify the emissivity values for the Hay-pasture land we have used a procedure as used by *Prata* [1994a]. We have varied ε and $\Delta\varepsilon$ within certain reliable limits ($\varepsilon > 0.95$ and $-0.015 < \Delta\varepsilon < 0.005$) and selected the combination which minimizes the error of the algorithm. For a given subset (satellite and passing time), changing the emissivity values modifies the bias, but the standard deviation remains constant. Thus the procedure of varying emissivity for minimizing the error could be only effective if the bias for different subsets are similar. If not, using a given emissivity combination which reduces the bias for one subset could result in the increasing of the bias for another subset. (As pointed out above, emissivity has been considered independent on the satellite and passing time.)

For our algorithm the optimum emissivity combination for the Hay-pasture land data set is $\varepsilon = 0.97$ and $\Delta\varepsilon = -0.010$, which yields $B(\varepsilon) = 2.4 \pm 0.3$ K ($\alpha = 51 \pm 3$ K and $\beta = 82 \pm 17$ K). This larger emissivity effect is in agreement with the results displayed in Figure 5. Here the offset values obtained for the linear regression are equal to $\Delta + B(\varepsilon)$, according to the split-window model of (1). Since Δ is independent of the surface, the results of Figure 5 show that the emissivity effect is about 1°C larger for the Hay-pasture land than for the Walpeup-fallow case. It can be also anticipated from Figure 5 that the lowest emissivity effect is for the wheat crop, as expected. The first row of Table 6 shows the statistics for the algorithm validation for the four subsets of the Hay test site. The first row of Table 7 gives the results grouped by satellite and also for the total data set. For the NOAA 11 daytime data set the worst results are obtained for the two points with $T_4 - T_5 \approx 3$°C, for which certain overestimation is found. As for the Walpeup-fallow surface, the NOAA 12 data give very different bias for the two overpass times.

For the Walpeup-bare soil we have taken $\varepsilon = 0.96$ and $\Delta\varepsilon = -0.010$ based on laboratory emissivity measurements of soil samples of the Walpeup site reported by *Prata* [1994b]. Thus the emissivity effect yielded $B(\varepsilon) = 3.0 \pm 0.4$ K ($\alpha = 52 \pm 4$ K and $\beta = 90 \pm 30$ K). The first row of Table 8 shows the algorithm validation statistics for the bare soil test site. For the daytime data, large overestimation and standard deviation was produced by the algorithm. As shown in section 6, most of the algorithms studied give large overestimation for the daytime data. However, the results for the nighttime data are satisfactory.

For the Walpeup-wheat crop we have selected $\varepsilon = 0.98$ and $\Delta\varepsilon = 0$, assuming a densely vegetated surface. Thus $\alpha = 53 \pm 5$ K, $\beta = 100 \pm 30$ K, and $B(\varepsilon) = 1.1 \pm 0.1$ K. The first row of Table 9 shows the results for the data set. The standard deviations are larger than for the previous surface types. This has been anticipated in the linear regression analysis performed over the database (see Table 2 and Figure 5) and may be due to the difficulties in measuring temperatures of complex crop-soil systems.

6. Algorithm Comparison

Several papers have recently addressed the comparison of AVHRR split-window algorithms using in situ LST measurements. However, most of them have used very limited data

Table 6. Validation Results for the Hay-Pasture Land Data Set

Hay-Pasture Land/NOAA 11 and 12	11/Daytime	11/Nighttime	12/Morning	12/Evening
This work	−0.1 ± 1.4	0.3 ± 0.8	−1.1 ± 0.9	0.9 ± 1.0
$\varepsilon = 0.97$, $\Delta\varepsilon = -0.010$	[−3.6, 2.0]	[−1.1, 1.9]	[−2.5, 1.1]	[−1.1, 2.2]
Price [1984]	−1.4 ± 1.9	1.0 ± 1.3	−1.5 ± 1.6	0.7 ± 1.3
$\varepsilon = 0.98$, $\Delta\varepsilon = -0.005$	[−5.6, 0.9]	[−1.4, 3.9]	[−4.5, 2.2]	[−2.8, 2.9]
Vidal [1991]	−0.7 ± 1.4	0.7 ± 1.1	−1.4 ± 1.3	0.7 ± 1.1
$\varepsilon = 0.97$, $\Delta\varepsilon = -0.005$	[−3.7, 1.1]	[−1.2, 3.2]	[−3.5, 1.8]	[−2.3, 2.5]
Kerr et al. [1992]	2.5 ± 1.1	3 ± 1	1.4 ± 1.1	3 ± 1
NA	[0.4, 4.3]	[1.6, 5.5]	[−0.1, 4.3]	[1.0, 5.1]
Ottlé and Vidal-Madjar [1992]	0.7 ± 1.0	1.2 ± 1.0	−0.5 ± 1.0	1.5 ± 1.0
$\varepsilon = 0.983$, $\Delta\varepsilon = -0.005$	[−0.9, 2.6]	[−0.4, 3.3]	[−1.9, 2.1]	[−0.6, 3.0]
Ulivieri et al. [1992]	0.3 ± 0.9	0.3 ± 0.9	−1.2 ± 0.9	0.8 ± 1.0
$\varepsilon = 0.96$, $\Delta\varepsilon = -0.015$	[−1.1, 2.2]	[−1.2, 2.2]	[−2.5, 1.2]	[−1.1, 2.1]
Prata [1993]	−0.8 ± 1.3	0.5 ± 1.1	−1.5 ± 1.3	0.6 ± 1.1
$\varepsilon = 0.97$, $\Delta\varepsilon = -0.010$	[−3.5, 1.0]	[−1.4, 3.0]	[−3.5, 1.6]	[−2.1, 2.5]
Sobrino et al. [1994]	−0.2 ± 1.1	0.5 ± 1.0	−1.2 ± 1.1	0.8 ± 1.0
$\varepsilon = 0.97$, $\Delta\varepsilon = -0.015$	[−2.1, 1.6]	[−1.2, 2.8]	[−2.7, 1.5]	[−1.5, 2.5]
Becker and Li [1995]	0.0 ± 1.0	0.6 ± 1.0	−1.0 ± 1.1	1.0 ± 1.0
$\varepsilon = 0.97$, $\Delta\varepsilon = -0.010$	[−1.9, 1.7]	[−1.1, 2.8]	[−2.4, 1.7]	[−2.4, 1.7]
François and Ottlé [1996]/*Q*	1.0 ± 1.4	1.4 ± 0.8	−0.1 ± 0.9	1.9 ± 1.0
$\varepsilon = 0.96$, $\Delta\varepsilon = 0$	[−2.5, 3.1]	[0.0, 3.1]	[−1.5, 2.2]	[−0.3, 3.3]
François and Ottlé [1996]/*W*	1.8 ± 0.9	0.9 ± 0.8	−0.2 ± 0.8	1.8 ± 0.9
$\varepsilon = 0.96$, $\Delta\varepsilon = 0$	[0.7, 3.9]	[−0.5, 2.5]	[−1.3, 1.7]	[−0.3, 3.2]

The mean error, the standard deviation, and the range of error are given in degrees Celsius. For each algorithm the emissivity values used are shown. NA, not applicable.

sets. *Cooper and Asrar* [1989] used four matchups of NOAA 9 and in situ measurements obtained with a handheld infrared radiometer to test *Price*'s [1984] algorithm over the First International Satellite Land Surface Climatology Project (ISLSCP) Field Experiment (FIFE) prairie in Kansas, obtaining an error of estimate for LST within ±3 K. For the same area, *Sugita and Brutsaert* [1993] have used a more extensive data set (63 matchups). They used potential temperatures and applied Price's algorithm assuming $\varepsilon = 1$ and $\Delta\varepsilon = 0$. More recently, *Kalluri and Dubayah* [1995] have used three matchup data from FIFE and tested the Price and the *Becker and Li* [1990] algorithms. *Caselles et al.* [1997c] have compared split-window algorithms using three data points from Hydrologic Atmospheric Pilot Experiment (HAPEX)-Sahel. A more extensive comparison, both for the size of the data set and the number of algorithms considered, has been published by *Prata et al.* [1995] using part of the Hay data set. The objective of this section is to complete the comparison by including all the validation data presented in the previous sections and some more recently published algorithms. The algorithms studied

Table 7. Summary of the Validation Results for the Hay-Pasture Land Data Set

Hay-Pasture Land/NOAA 11 and 12 (Summary)	NOAA 11	NOAA 12	All Data
This work	0.1 ± 1.1	−0.3 ± 1.4	−0.1 ± 1.2
$\varepsilon = 0.97$, $\Delta\varepsilon = -0.010$	[−3.6, 2.0]	[−2.5, 2.2]	[−3.6, 2.2]
Price [1984]	0.1 ± 1.9	−0.6 ± 1.8	−0.3 ± 1.9
$\varepsilon = 0.98$, $\Delta\varepsilon = -0.005$	[−5.6, 3.9]	[−4.5, 2.9]	[−5.6, 3.9]
Vidal [1991]	0.1 ± 1.4	−0.5 ± 1.6	−0.2 ± 1.5
$\varepsilon = 0.97$, $\Delta\varepsilon = -0.005$	[−3.7, 3.2]	[−3.5, 2.5]	[−3.7, 3.2]
Kerr et al. [1992]	3 ± 1	2.3 ± 1.5	3 ± 1
NA	[0.4, 5.5]	[−0.1, 5.1]	[−0.1, 5.5]
Ottlé and Vidal-Madjar [1992]	1.0 ± 1.0	0.4 ± 1.4	0.7 ± 1.3
$\varepsilon = 0.983$, $\Delta\varepsilon = -0.005$	[−0.9, 3.3]	[−1.9, 3.0]	[−1.9, 3.3]
Ulivieri et al. [1992]	0.3 ± 0.9	−0.4 ± 1.4	−0.1 ± 1.0
$\varepsilon = 0.96$, $\Delta\varepsilon = -0.015$	[−1.2, 2.2]	[−2.5, 2.1]	[−2.5, 2.2]
Prata [1993]	0.0 ± 1.3	−0.6 ± 1.6	−0.3 ± 1.5
$\varepsilon = 0.97$, $\Delta\varepsilon = -0.010$	[−3.5, 3.0]	[−3.5, 2.5]	[−3.5, 3.0]
Sobrino et al. [1994]	0.2 ± 1.1	−0.3 ± 1.5	−0.1 ± 1.3
$\varepsilon = 0.97$, $\Delta\varepsilon = -0.015$	[−2.1, 2.8]	[−2.7, 2.5]	[−2.7, 2.8]
Becker and Li [1995]	0.4 ± 1.0	−0.2 ± 1.4	0.1 ± 1.3
$\varepsilon = 0.97$, $\Delta\varepsilon = -0.010$	[−1.9, 2.8]	[−2.4, 2.6]	[−2.4, 2.8]
François and Ottlé [1996]/*Q*	1.2 ± 1.1	0.8 ± 1.4	1.0 ± 1.3
$\varepsilon = 0.96$, $\Delta\varepsilon = 0$	[−2.5, 3.1]	[−1.5, 3.3]	[−2.5, 3.3]
François and Ottlé [1996]/*W*	1.3 ± 1.0	0.7 ± 1.3	1.0 ± 1.2
$\varepsilon = 0.96$, $\Delta\varepsilon = 0$	[−0.5, 3.9]	[−1.3, 3.2]	[−1.3, 3.9]

The mean error, the standard deviation, and the range of error are given in degrees Celsius. For each algorithm the emissivity values used are shown.

Table 8. Validation Results for the Walpeup-Bare Soil Data Set

	$\varepsilon = 0.96, \Delta\varepsilon = -0.010$		
Walpeup-Bare Soil/NOAA 11	Daytime	Nighttime	All Data
This work	−3 ± 2	−0.1 ± 0.7	−1.3 ± 1.9
	[−6.2, −0.4]	[−1.6, 1.6]	[−6.2, 1.6]
Price [1984]	−6 ± 2	−1.5 ± 0.9	−4 ± 3
	[−8.8, −2.8]	[−3.2, 0.2]	[−8.8, 0.2]
Vidal [1991]	−5 ± 1	−1.9 ± 0.7	−3 ± 2
	[−6.9, −2.7]	[−3.5, −0.5]	[−6.9, −0.5]
Kerr et al. [1992]	−1.7 ± 1.0	0.2 ± 0.7	0.6 ± 1.2
	[−3.1, −0.2]	[−1.4, 1.6]	[−3.1, 1.6]
Ottlé and Vidal-Madjar [1992]	−2.3 ± 1.1	−1.3 ± 0.7	−1.7 ± 1.0
	[−4.1, −0.4]	[−2.8, 0.4]	[−4.1, 0.4]
Ulivieri et al. [1992]	−0.7 ± 1.0	0.6 ± 0.7	0.1 ± 1.0
	[−2.2, 0.5]	[−1.0, 2.1]	[−2.2, 2.1]
Prata [1993]	−4 ± 1	−0.5 ± 0.7	−1.8 ± 1.9
	[−5.4, −1.3]	[−2.1, 0.9]	[−5.4, 0.9]
Sobrino et al. [1994]	−2.0 ± 1.2	0.3 ± 0.7	−0.7 ± 1.5
	[−3.7, −0.4]	[−1.3, 1.7]	[−3.7, 1.7]
Becker and Li [1995]	−2.3 ± 1.2	−0.1 ± 0.7	−1.1 ± 1.5
	[−4.0, −0.8]	[−1.8, 1.4]	[−4.0, 1.4]
François and Ottlé [1996]/*Q*	−1.2 ± 1.7	1.4 ± 0.6	0.3 ± 1.8
	[−4.5, 1.2]	[−0.1, 3.0]	[−4.5, 3.0]
François and Ottlé [1996]/*W*	1.0 ± 1.3	1.2 ± 0.8	1.1 ± 1.0
	[−0.9, 3.8]	[−0.4, 3.0]	[−1.7, 6.9]

The mean error, the standard deviation, and the range of error are given in degrees Celsius.

are given in Table 10, while the validation results have been shown in Tables 3–9.

6.1.1. *Price* [1984]. The comparison with the CMS SST data shows an overestimation of the surface temperature in the two emissivity cases considered (see Table 3). The quite large difference between the blackbody case and the $\varepsilon = 0.99$ and $\Delta\varepsilon = 0.004$ case indicates that the emissivity effect may also be overestimated. For the land surfaces, large inconsistencies have been found in the bias between the different passing times over a given surface.

6.1.2. *Becker and Li* [1990, 1995]. When applied to the CMS SST data (Table 3), this algorithm gives an overestimation of 1.6°C for both emissivity cases. Moreover, the results obtained by *Prata et al.* [1995] in the comparison with LST data were not satisfactory. A similar overestimation of 1.5°C has been observed by the authors for different data sets, which have led them to propose a new algorithm [*Becker and Li*, 1995]. This algorithm keeps the form of the 1990 algorithm but expresses the numerical coefficients as linear functions of the atmospheric water vapor content W (see Table 10).

Table 9. Validation Results for the Walpeup-Wheat Crop Data Set

	$\varepsilon = 0.98, \Delta\varepsilon = 0$		
Walpeup-Wheat Crop/NOAA 11	Daytime	Nighttime	All Data
This work	−0.1 ± 2.1	0.2 ± 1.4	0.1 ± 1.7
	[−4.3, 3.7]	[−3.0, 3.4]	[−4.3, 3.7]
Price [1984]	−1.8 ± 2.2	0.5 ± 1.6	−0.5 ± 2.2
	[−6.4, 2.1]	[−3.0, 4.0]	[−6.4, 4.0]
Vidal [1991]	−0.4 ± 2	0.7 ± 1.5	0.2 ± 1.8
	[−4.3, 3.2]	[−2.5, 3.9]	[−4.3, 3.9]
Kerr et al. [1992]	3 ± 2	4 ± 2	4 ± 2
	[−0.3, 7.2]	[1.0, 7.2]	[−0.3, 7.2]
Ottlé and Vidal-Madjar [1992]	−0.3 ± 2.1	−0.1 ± 1.5	−0.2 ± 1.7
	[−3.6, 3.8]	[−3.2, 2.7]	[−3.6, 3.8]
Ulivieri et al. [1992]	1.6 ± 2.2	0.8 ± 1.4	1.2 ± 1.8
	[−1.9, 6.2]	[−2.3, 4.1]	[−2.3, 6.2]
Prata [1993]	0.0 ± 2.0	0.6 ± 1.5	0.4 ± 1.8
	[−3.8, 3.6]	[−2.6, 3.6]	[−3.6, 3.8]
Sobrino et al. [1994]	0.5 ± 2.1	0.6 ± 1.5	0.6 ± 1.8
	[−2.8, 4.9]	[−2.6, 3.6]	[−2.8, 4.9]
Becker and Li [1995]	0.3 ± 2.1	0.6 ± 1.5	0.4 ± 1.8
	[−3.3, 4.6]	[−2.7, 3.6]	[−3.3, 4.6]
François and Ottlé [1996]/*Q*	−2 ± 4	0.9 ± 1.4	0 ± 3
	[−13.3, 3.5]	[−2.3, 3.4]	[−13.3, 3.5]
François and Ottlé [1996]/*W*	3 ± 3	0.8 ± 1.4	1.7 ± 2.3
	[−1.2, 9.1]	[−2.6, 5.0]	[−2.6, 9.1]

The mean error, the standard deviation, and the range of error are given in degrees Celsius.

Table 10. Split-Window Algorithms

Author	Algorithm
Price [1984]	$T = [T_4 + 3.33(T_4 - T_5)]((5.5 - \varepsilon_4)/4.5) - 0.75T_5\Delta\varepsilon$
Becker and Li [1990]	$T = 1.274 + (1 + 0.15616\ (1 - \varepsilon)/\varepsilon - 0.482\ \Delta\varepsilon/\varepsilon^2)\ (T_4 + T_5)/2 + (6.26 + 3.98\ [(1-\varepsilon)/\varepsilon] + 38.33\ (\Delta\varepsilon/\varepsilon^2)\ [(T_4 - T_5)/2])$
Vidal [1991]	$T = T_4 + 2.78(T_4 - T_5) + 50\ [(1 - \varepsilon)/\varepsilon] - 300\ (\Delta\varepsilon/\varepsilon)$
Kerr et al. [1992][a]	$T = P_v[T_5 + 2.6(T_4 - T_5) - 2.4] + (1 - P_v)[T_4 + 2.1(T_4 - T_5) + 3.1]$
Ottlé and Vidal-Madjar [1992][b]	$T = a_0 + a_1T_4 + a_2T_5$
Ulivieri et al. [1992]	$T = T_4 + 1.8(T_4 - T_5) + 48(1 - \varepsilon) - 75\Delta\varepsilon$
Prata [1993][c]	$T = (3.42/\delta)\ T_4 - (2.42/\delta)\ T_5 + ([1 - \delta]/\delta)\ [(B_4(T_4) - \Delta I\downarrow)\ (\partial B_4/\partial T)^{-1}_{T_4} - T_4]$ $\delta = \varepsilon_4 + 2.42\tau_5\Delta\varepsilon$
Sobrino et al. [1994][d]	$B_4(T) = (\alpha_1 + \alpha_2/R)\ B_4(T_4) + (\alpha_3 + \alpha_4/R)B_5(T_5) + (\alpha_5 + \alpha_6/R)$ $R = \tau_5/\tau_4$ $\alpha_i = \alpha_{i0} + \alpha_{i1}(1 - \varepsilon_4) + \alpha_{i2}\Delta\varepsilon$
Becker and Li [1995][e]	$T = (-7.491 - 0.407W) + [1.0290 + (0.2106 - 0.0307\ W \cos\theta)(1 - \varepsilon_4) - (0.3696 - 0.737W)\Delta\varepsilon]\ (T_4 + T_5)/2 + [4.25 + 0.56W + (3.41 + 1.59W)(1 - \varepsilon_4) - (23.85 - 3.89W)\Delta\varepsilon]\ (T_4 - T_5)/2$
François and Ottlé [1996]/Q[f]	$T = T_4 + a(T_4 - T_5) + b(T_4 - T_5)^2 + c$
François and Ottlé [1996]/W[g]	$T = a'(W)T_4 + b'(W)T_5 + c'(W)$

[a] P_v is the vegetation proportion in the pixel.
[b] The parameters a_0, a_1, and a_2 are numeric coefficients tabulated for several emissivity combinations.
[c] B_i is the Planck function weighted for AVHRR channel i, and $\Delta I\downarrow = 6$ mW/(m^2 cm^{-1} sr).
[d] The parameters α_{i0}, α_{i1} and α_{i2} are numeric coefficients given by the authors.
[e] W is the atmospheric water vapor content in grams per square centimeter.
[f] The parameters a, b, and c are numeric coefficients tabulated for different emissivity values.
[g] The parameters $a'(W)$, $b'(W)$, and $c'(W)$ are quadratic functions of the water vapor content, with the numeric coefficients tabulated for different emissivity values.

The *Becker and Li* [1990] algorithm has been substituted hereafter by the 1995 version for the LST data comparison. To apply this algorithm, the mean monthly climatological values of W given by *Prata* [1994b] have been used. The results obtained are shown in Tables 4–9.

6.1.3. *Vidal* [1991]. The application to the CMS SST data set gives acceptable results, although a large difference is observed between the bias for the two sea surface emissivity cases considered. This indicates that the emissivity effect is overestimated, likely due to the very high value of the coefficient of the $\Delta\varepsilon$ term (see Table 10). For the LST data, large differences are found between satellite passing times for the same surfaces.

6.1.4. *Kerr et al.* [1992]. The algorithm has not been applied to the SST data. For LST it requires the specification of the vegetation proportion P_v (see Table 10). We have used $P_v = 0.5$ for the Walpeup-fallow and Hay-pasture land data sets, $P_v = 0$ for the Walpeup-bare soil data set, and $P_v = 1$ for the Walpeup-wheat crop data set. Results show large underestimation of the in situ LST.

6.1.5. *Ottlé and Vidal-Madjar* [1992]. This algorithm uses different constant coefficients tabulated for several surface emissivity combinations. Not all possible combinations were considered by the authors. In the present study, we have selected the coefficients corresponding to the emissivity combinations closest to the assigned values for each surface type. For the SST data, only the case $\varepsilon = 1$ and $\Delta\varepsilon = 0$ is possible. For the Walpeup-fallow and Hay data the best possible combination is $\varepsilon_4 = 0.98$ and $\varepsilon_5 = 0.985$. For the Walpeup-bare soil we had to use the $\varepsilon_4 = 0.96$ and $\varepsilon_5 = 0.98$ as the closest choice. Finally, for the Walpeup-wheat crop case we have used the appropriate combination ($\varepsilon_4 = \varepsilon_5 = 0.98$).

6.1.6. *Ulivieri et al.* [1992]. This algorithm usually underestimates LSTs for the data studied here. For the Hay-pasture land case the best emissivity combination found is $\varepsilon = 0.96$ and $\Delta\varepsilon = -0.015$, which is nearly at the extreme of the range considered.

6.1.7. *Prata* [1993]. The numerical coefficients of the algorithm were calculated using radiosonde measurements for the Walpeup area. For the Walpeup-fallow and Hay-pasture land surfaces the algorithm yields different biases depending on the satellite passing time.

6.1.8. *Sobrino et al.* [1994]. This algorithm uses radiances instead of temperatures and introduces the parameter $R = \tau_5/\tau_4$ to account for the atmospheric variability (see Table 10). The *Becker and Li* [1995] algorithm is similar to this formulation, since the R parameter is closely related to W and can be calculated using the spatial variations of the brightness temperatures T_4 and T_5 [*Sobrino et al.*, 1994]. In the present study, the procedure for retrieving W from satellite data cannot be applied. Instead, we have used the monthly mean values of τ_4 and τ_5 tabulated by *Prata* [1994b]. Application has not been possible for the CMS SST data. Very similar results are shown in Tables 4–9 for the *Sobrino et al.* [1994] and *Becker and Li* [1995] algorithm. In fact, both algorithms have been derived using the same simulated database. For the Hay data the rather extreme value $\Delta\varepsilon = -0.015$ has been used for the *Sobrino et al.* [1994] algorithm.

6.1.9. *François and Ottlé* [1996]. Two different algorithms have been proposed by *François and Ottlé* [1996] with the aim of accounting for the atmospheric variability of the split-window coefficients. The first is a quadratic algorithm in $T_4 - T_5$ (labeled Q in Tables 3–10), whereas the second includes water vapor dependent coefficients (labeled W). The numeric coefficients for both equations were tabulated as functions of the surface emissivity. However, only gray body surfaces ($\varepsilon_4 = \varepsilon_5$) were considered by the authors. Application of the W algorithm is not possible for the CMS SST database. For the LST database the water vapor data from *Prata* [1994b] have been used. An overall underestimation of the LST is obtained

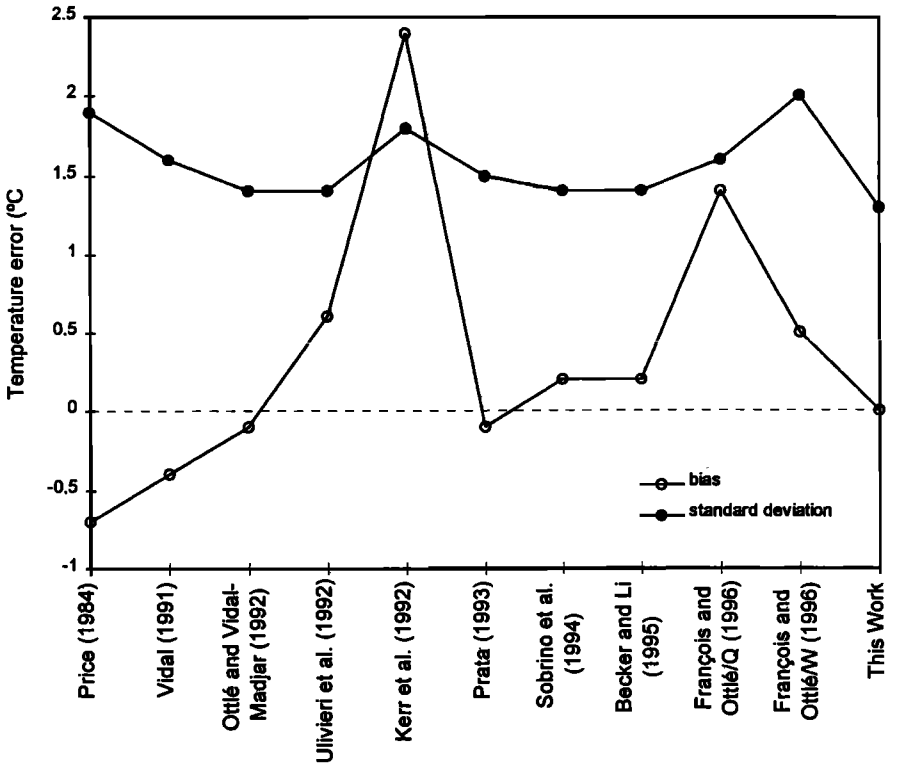

Figure 6. Bias and standard deviation for the algorithms studied over the total LST data set.

for both algorithms. For the Hay-pasture land data it is apparent that there is a need to take into account the spectral variation of emissivity. However, even for the Walpeup-wheat crop data (Table 9), where no spectral effects are expected, the results yielded large error ranges and standard deviations.

7. Discussion

The algorithm comparison of the preceding section is an example of the importance of the coefficient specification and the algorithm form in the LST determination. As a summary, Figure 6 shows the mean error and the standard deviation obtained for each algorithm over the total LST database (358 data). The empirical algorithms (derived from coincident in situ and AVHRR measurements of LST) as those of *Vidal* [1991] and *Kerr et al.* [1992] have shown poor performance when applied to the validation data sets. These algorithms were derived with very limited data, both in terms of the number of measurements and the atmospheric and surface types considered. The results shown in this paper indicate that the application to other atmospheres and surfaces with different characteristics may not be possible. Similar consequences can be obtained for the *Price* [1984] algorithm. This model can be considered as semiempirical since one of its coefficients ($A = 3.33$) was obtained from brightness temperature variances for one actual AVHRR image. For this case, and also for *Vidal* [1991] with $A = 2.78$, the large value for this coefficient seems to be the reason for a systematic overestimation of both the SST and LST data. Besides, both algorithms show too much sensitivity to emissivity values.

Most of the algorithms studied in this paper were derived from numerical simulation [*Ottlé and Vidal-Madjar*, 1992; *Ulivieri et al.*, 1992; *Sobrino et al.*, 1994; *Becker and Li*, 1995; *François and Ottlé*, 1996]. The algorithm of *Prata* [1993] follows a different approach, since the theoretically derived coefficients are calculated and regionally adjusted by using actual radiosonde measurements or climatological profiles. In general, there is agreement in the necessity of adjusting the algorithms according to the atmospheric characteristics. In the case of *Ottlé and Vidal-Madjar* [1992] and *Ulivieri et al.* [1992], simple linear algorithms applicable to midlatitude conditions were proposed. In the first case, an additional problem is the insufficiency in the parameterization of the emissivity effect. The algorithms of *François and Ottlé* [1996] suffer from the same limitations, as only gray body surfaces were considered.

The algorithms of *Sobrino et al.* [1994] and *Becker and Li* [1995] include explicitly the atmospheric dependence in the algorithms. These models are nearly equivalent, since both were derived from the same simulation database and have similar structure. Moreover, they rely upon the determination of the transmittance ratio R or the atmospheric water vapor content W to account for the atmospheric variability of the split-window equations. These parameters are included in all the coefficients of the algorithms. Then, the performance of both formulations is highly dependent on the errors in the determination of R and W, respectively. The algorithm proposed in this paper also requires the knowledge of the atmospheric humidity but only for the emissivity correction coefficients α and β. Even in this case, a climatological estimate of W is sufficient, and the atmospheric dependence of the algorithm is mainly based on the simple quadratic dependence on $T_4 - T_5$. The use of more complicated formulations based on the determination of R and W has demonstrated no improvement over the simpler quadratic algorithm.

There seems to be some error associated with time of day of

the data. For the NOAA 12 data sets the proposed algorithm has shown notable discrepancy between the morning and evening passing times. This problem has been noticed for all of the algorithms analyzed, and many of them also give large differences between daytime and nighttime NOAA 11 data. There are two possible causes: (1) the algorithms need different specifications for different time of day conditions, and (2) there exist errors in the in situ data, which are probably correlated with time of day. The great difficulties in making in situ LST measurements should be pointed out, and the validation data can be questioned in this regard.

8. Conclusions

The results obtained in the preceding sections indicate that LST can be derived from AVHRR data with accuracies better than ±2 K using certain split-window algorithms. To this end, two main requirements need to be accomplished.

First, it is necessary to specify the surface emissivities in the AVHRR channels. In this paper we have used field and laboratory measurements reported by *Prata* [1994b] together with some guess and hypotheses according to the nature of the surfaces under consideration. This procedure has proved to be successful, as shown by the validation results. As an advantage of the 10–12.5 μm window, emissivities of natural surfaces are usually high and with low spectral variation. However, it is not sufficient to use a constant gray body emissivity value. At pixel scale the effective emissivity depends mostly on the fraction of vegetation cover, the background type, and the geometrical distribution of the vegetation. Taking these factors into account, the effective emissivity for partially covered surfaces can be modeled as proposed by *Valor and Caselles* [1996] for most applications of LST. This simple, operational method, which is an intermediate solution to the emissivity estimation problem, is more accurate than using a single emissivity value for extended areas.

Second, the coefficients of the split-window algorithms need to be correctly specified, taking into account the atmospheric variability existing at global scale. The algorithm proposed here (equation (11)) uses a set of coefficients which have been derived using SST matchups. This ensures that the coefficients have been calibrated with actual data, and therefore certain credit can be relied upon them. In addition, the procedure can be also useful for the new generation of thermal infrared sensors to be launched in the near future. The validation results, both for the CMS SST and the LST databases, give more confidence on the suitability of the algorithm. For the LST data, standard errors (rmsd) of ±1.0–1.5 K and no significant bias have been found for most cases. Although the performance of the algorithm proposed is encouraging, more validation studies with different data sets are required. The LST data sets used in this paper encompassed certain variability in surface types, with bare soils, sparse vegetation, and developed crops. The variability in surface temperatures was also considerable, with values from 0° to 50°C. However, the atmospheric conditions were very uniform, namely low water vapor content with small seasonal variation. Therefore, the conclusions of the paper are limited to dry atmospheres. In moist atmospheric conditions, worse algorithm performances are expected. In fact, using a reduced HAPEX-Sahel database, rmsd errors of ±2 K were reported by *Caselles et al.* [1997c] using a previous version of (11). Nevertheless, more validation works are required in moist atmospheric conditions.

Acknowledgments. The authors wish to express their gratitude to J. Vázquez (Jet Propulsion Laboratory) for assistance with the NOAA-NASA Pathfinder Matchup Database. We are also indebted to F. Prata (CSIRO, Australia) for supplying LST data and to P. Le Borgne (Centre de Météorologie Spatiale, Lannion, France) for the SST data. Constructive suggestions of the reviewers are also acknowledged. This research was supported by the EC Environment and Climate Research Programme (contract ENV4-CT95-0166, Climatology and Natural Hazards) and by the Spanish Comisión Interministerial de Ciencia y Tecnología (project reference AMB94-1208).

References

Antoine, J. Y., M. Derrien, L. Harang, P. Le Borgne, H. Le Gleau, and C. Le Goas, Errors at large satellite zenith angles on AVHRR derived sea surface temperatures, *Int. J. Remote Sens.*, *15*, 1797–1804, 1992.

Becker, F., and Z.-L. Li, Towards a local split-window method over land surfaces, *Int. J. Remote Sens.*, *11*, 369–394, 1990.

Becker, F., and Z.-L. Li, Surface temperature and emissivity at various scales: Definition, measurement and related problems, *Remote Sens. Rev.*, *12*, 225–253, 1995.

Caselles, V., J. A. Sobrino, and C. Coll, A physical model for interpreting the land surface temperature obtained by remote sensors over incomplete canopies, *Remote Sens. Environ.*, *39*, 203–211, 1992.

Caselles, V., C. Coll, E. Valor, and E. Rubio, Thermal band selection for the PRISM instrument, 2, Analysis and comparison of the existing atmospheric and emissivity correction methods for land surface temperature, *J. Geophys. Res.*, in press, 1997a.

Caselles, V., E. Valor, C. Coll, and E. Rubio, Thermal band selection for the PRISM instrument, 1, Analysis of emissivity-temperature separation algorithms, *J. Geophys. Res.*, in press, 1997b.

Caselles, V., C. Coll, and E. Valor, Land surface emissivity and temperature determination in the whole HAPEX-Sahel area from AVHRR data, *Int. J. Remote Sens.*, *18*, 1009–1027, 1997c.

Coll, C., and V. Caselles, Analysis of the atmospheric and emissivity influence on the split-window equation for sea surface temperature, *Int. J. Remote Sens.*, *15*, 1915–1932, 1994.

Coll, C., V. Caselles, J. A. Sobrino, and E. Valor, On the atmospheric dependence of the split-window equation for land surface temperature, *Int. J. Remote Sens.*, *15*, 105–122, 1994.

Cooper, D. I., and G. Asrar, Evaluating atmospheric correction models for retrieving surface temperatures from the AVHRR over a tallgrass prairie, *Remote Sens. Environ.*, *27*, 93–102, 1989.

François, C., and C. Ottlé, Atmospheric corrections in the thermal infrared: Global and water vapor dependent split-window algorithms—Applications to ATSR and AVHRR data, *IEEE Trans. Geosci. Remote Sens.*, *34*, 457–469, 1996.

Kalluri, S. N. V., and R. O. Dubayah, Comparison of atmospheric correction models for thermal bands of the advanced very high resolution radiometer over FIFE, *J. Geophys. Res.*, *100*(D12), 25,411–25,418, 1995.

Kerr, Y. H., J. P. Lagouarde, and J. Imbernon, Accurate land surface temperature retrieval from AVHRR data with the use of an improved split-window algorithm, *Remote Sens. Environ.*, *41*, 197–209, 1992.

Masuda, K., T. Takashima, and Y. Takayama, Emissivity of pure and sea waters for the model sea surface in the infrared window regions, *Remote Sens. Environ.*, *24*, 313–329, 1988.

Maul, G. A., Zenith angle effects in multichannel infrared sea surface sensing, *Remote Sens. Environ.*, *13*, 439–451, 1983.

May, D. A., Global and regional comparative performance of linear and non-linear satellite multichannel sea surface temperature algorithms, *Tech. Rep. NRL/MR/7240-93-7049*, Nav. Res. Lab., Stennis Space Cent., Miss., 1993.

May, D. A., and R. J. Holyer, Sensitivity of satellite multichannel sea surface temperature retrievals to the air-sea temperature difference, *J. Geophys. Res.*, *98*(C7), 12,567–12,577, 1993.

McClain, E. P., W. G. Pichel, and C. C. Walton, Comparative performance of AVHRR-based multichannel sea surface temperatures, *J. Geophys. Res.*, *90*(C6), 11,587–11,601, 1985.

McMillin, L. M., Estimation of sea surface temperatures from two infrared window measurements with different absorption, *J. Geophys. Res.*, *80*(C36), 5113–5117, 1975.

Norman, J. M., M. Divakarla, and N. S. Goel, Algorithms for extracting information from remote thermal-IR observations of Earth's surface, *Remote Sens. Environ.*, *51*, 157–169, 1995.

Ottlé, C., and D. Vidal-Madjar, Estimation of land surface temperature with NOAA-9 data, *Remote Sens. Environ.*, *40*, 27–41, 1992.

Platt, C. M. R., and A. J. Prata, Nocturnal effects in the retrieval of land surface temperatures from satellite measurements, *Remote Sens. Environ.*, *45*, 127–136, 1993.

Podestá, G., S. Shenoi, J. M. Brown, and R. H. Evans, AVHRR pathfinder oceans matchup database 1985–1993 (version 18), Rosenstiel Sch. of Mar. and Atmos. Sci., Univ. of Miami, Miami, Fla., 1995.

Prata, A. J., Land surface temperatures derived from the advanced very high resolution radiometer and the along track scanning radiometer, 1, Theory, *J. Geophys. Res.*, *98*(D9), 16,689–16,702, 1993.

Prata, A. J., Land surface temperatures derived from the advanced very high resolution radiometer and the along track scanning radiometer, 2, Experimental results and validation of AVHRR algorithms, *J. Geophys. Res.*, *99*(D6), 13,025–13,058, 1994a.

Prata, A. J., Validation data for land surface temperature determination from satellites, *Pap. 33*, 36 pp., Div. of Atmos. Res., Commonw. Sci. and Ind. Res. Org., Melbourne, Victoria, Australia, 1994b.

Prata, A. J., V. Caselles, C. Coll, J. A. Sobrino, and C. Ottlé, Thermal remote sensing of land surface temperature from satellites: Current status and future prospects, *Remote Sens. Rev.*, *12*, 175–224, 1995.

Price, J. C., Land surface temperature measurements from the split-window channels of the NOAA 7 AVHRR, *J. Geophys. Res.*, *89*(D5), 7231–7237, 1984.

Rubio, E., V. Caselles, and C. Badenas, Emissivity measurements of several soils and vegetation types in the 8–14 μm waveband: Analysis of two field methods, *Remote Sens. Environ.*, *59*, 490–521, 1997.

Salisbury, J. W., and D. M. D'Aria, Emissivity of terrestrial materials in the 8–14 μm atmospheric window, *Remote Sens. Environ.*, *42*, 83–106, 1992.

Schluessel, P., W. J. Emery, H. Grassl, and T. Mammen, On the bulk-skin temperature difference and its impact on satellite remote sensing of sea surface temperature, *J. Geophys. Res.*, *95*(C8), 13,341–13,356, 1990.

Schmugge, T. J., F. Becker, and Z.-L. Li, Spectral emissivity variations observed in airborne surface temperature measurements, *Remote Sens. Environ.*, *35*, 95–104, 1991.

Sobrino, J. A., C. Coll, and V. Caselles, Atmospheric correction for land surface temperature using NOAA-11 AVHRR channels 4 and 5, *Remote Sens. Environ.*, *38*, 19–34, 1991.

Sobrino, J. A., Z.-L. Li, M.-P. Stoll, and F. Becker, Improvements in the split-window technique for land surface temperature determination, *IEEE Trans. Geosci. Remote Sens.*, *32*, 243–253, 1994.

Strong, A. E., and E. P. McClain, Improved ocean temperatures from space-comparison with drifting buoys, *Bull. Am. Meteorol. Soc.*, *65*, 138–142, 1984.

Sugita, M., and W. Brutsaert, Comparison of land surface temperatures derived from satellite observations with ground truth during FIFE, *Int. J. Remote Sens.*, *14*, 1659–1676, 1993.

Ulivieri, C., M. M. Castronuovo, R. Francioni, and A. Cardillo, A split-window algorithm for estimating land surface temperatures from satellites, COSPAR, Comm. on Space Programs and Res., Washington, D. C., Aug. 27 to Sept. 5, 1992.

Valor, E., and V. Caselles, Mapping land surface emissivity from NDVI: Application to European, African and South American areas, *Remote Sens. Environ.*, *57*, 167–184, 1996.

Vidal, A., Atmospheric and emissivity correction of land surface temperature measured from satellite using ground measurements or satellite data, *Int. J. Remote Sens.*, *12*, 2449–2460, 1991.

Walton, C. C., Nonlinear multichannel algorithms for estimating sea surface temperature with AVHRR satellite data, *J. Appl. Meteorol.*, *27*, 115–124, 1988.

Walton, C. C., E. P. McClain, and J. F. Sapper, Recent changes in satellite based multi-channel sea surface temperature algorithms, Paper presented at Science and Technology for a New Oceans Decade, Mar. Technol. Soc., Washington, D. C., 1990.

Wan, Z., and J. Dozier, Land surface temperature measurement from space: Physical principles and inverse modeling, *IEEE Trans. Geosci. Remote Sens.*, *27*, 268–278, 1989.

V. Caselles and C. Coll, Department of Thermodynamics, Faculty of Physics, University of Valencia, 46100 Burjassot, Valencia, Spain. (e-mail: cesar.coll@uv.es)

(Received September 20, 1996; revised March 14, 1997; accepted March 26, 1997.)